



Escola d'Enginyeria de Telecomunicació i  
Aeroespacial de Castelldefels

UNIVERSITAT POLITÈCNICA DE CATALUNYA

# TREBALL FINAL DE GRAU

**TÍTOL DEL TFG:** Implementation of a point merge system based arrival at Berlin-Schönefeld airport

**TITULACIÓ:** Grau en Enginyeria d'Aeronavegació

**AUTOR:** Alfonso Pelegrín Rellán

**DIRECTOR:** Raúl Sáez García

**DATA:** 04/02/2020

## Resum

En aquest projecte s'ha estudiat i proposat un disseny per la implementació d'un nou procediment d'arribades anomenat Point Merge System (PMS) a l'aeroport de Berlin-Schönefeld, per tal d'estudiar la possibilitat de permetre a les aeronaus realitzar operacions de descens continu (CDO). El PMS permet reduir les esperes dels avions mitjançant una millor fusió del flux de vols d'arribada; conseqüentment, es redueix l'impacte mediambiental dels vols donat que estan menys temps a l'aire. A més, les CDOs permeten a les aeronaus fer descensos molt més eficients, reduint el consum de combustible i el soroll.

Un disseny de PMS s'ha proposat per la pista 07L de l'aeroport de Berlin-Schönefeld aprofitant la STAR actual. Tenint en compte que el tràfic d'arribada per aquesta pista es fusiona a un IAF per totes les arribades del nord i en un altre IAF per les de sud, s'ha decidit aplicar un únic PMS compost per dos arcs, un serà utilitzat pel tràfic del nord i l'altre pel tràfic del sud.

En aquest disseny s'ha tingut en compte totes les mesures i regulacions imposades per EUROCONTROL per tal d'assegurar la seguretat en les operacions. Finalment s'ha pogut concloure que l'aeroport de Berlin-Schönefeld està capacitat per la implementació d'un PMS i poder beneficiar-se dels seus avantatges.

En aquest treball també s'ha estudiat l'efecte de diferents paràmetres sobre la eficiència al volar CDOs. Les trajectòries necessàries per aquests càlculs s'han generat amb un optimitzador de trajectòries on el model de performances dels avions s'ha obtingut del Base of Aircraft Data (BADA) d'EUROCONTROL.

Els resultats obtinguts mostren que a mida que l'aeronau vola amb un cost índex més elevat la velocitat augmenta, arribant així abans a la pista d'aterratge, però el consum de fuel també augmenta. Quant al consum de fuel, es pot concloure que donat que els avions realitzen CDOs s'aconsegueix una molt millor eficiència de combustible respecte als procediments convencionals.

Per resumir, la implementació d'un PMS a l'aeroport de Berlin-Schönefeld és possible i permetria a l'aeroport i a les aerolínies beneficiar-se de tots els seus avantatges.

## Overview

This project assesses the implementation of an innovative arrival procedure, called Point Merge System (PMS), at Berlin-Schönefeld airport. The viability of performing continuous descend operations (CDO) in such kind of system has been addressed. The PMS reduces the delay of aircraft through a better arrival flow merge and it reduces the environmental impact of the flights since they stay less time on air. Furthermore, CDOs allow aircraft to perform more efficient descents, with a reduction in both fuel consumption and noise nuisance.

A design of a PMS has been proposed for the runway 07L of Berlin-Schönefeld airport using the current STAR. Since the arrival traffic for this runway merges at one IAF for the north arrivals and another for the south ones, it has been decided to apply a single PMS composed by two arcs; one will be used by the north traffic and the other one by the south traffic.

In this design it has been taken into consideration all the regulations and measures imposed by EUROCONTROL in order to keep the safety of the operations. Finally, it has been concluded that a PMS could be implemented at Berlin-Schönefeld.

In this project the effect of several parameters on the efficiency when flying CDOs has been studied. The trajectories needed for these computations have been generated with a trajectory optimizer where the aircraft performance model is obtained from the Base of Aircraft Data (BADA) by EUROCONTROL.

The results obtained show that the higher the cost index the higher the speed of the aircraft is, which means an earlier time of arrival at the runway; however, the fuel consumption increases as well. Regarding the fuel consumption, it can be said that given the fact that the aircraft perform CDOs a better fuel efficiency is achieved than with conventional procedures.

To sum up, the implementation of a PMS procedure at Berlin-Schönefeld is possible and would give many benefits to the airport and the airlines involved.

# INDEX

<b>INTRODUCTION .....</b>	<b>1</b>
<b>CHAPTER 1. OPERATIONAL CONTEXT .....</b>	<b>3</b>
1.1 <b>Airspace and control phases .....</b>	<b>3</b>
1.2 <b>Air traffic control tasks .....</b>	<b>4</b>
1.3 <b>Integration of arrivals .....</b>	<b>4</b>
1.3.1 Convergence versus spacing .....	4
1.3.2 Intermediate and final sequences .....	5
1.3.3 Phases in sequence management .....	6
1.3.4 Lateral path stretching or shortening .....	6
1.4 <b>Conventional operating methods .....</b>	<b>7</b>
1.4.1 Advanced procedures and tools .....	7
1.5 <b>Continuous descend operations .....</b>	<b>9</b>
<b>CHAPTER 2. THE POINT MERGE SYSTEM .....</b>	<b>11</b>
2.1 <b>Point Merge System History .....</b>	<b>11</b>
2.2 <b>Current applications of the point merge concept .....</b>	<b>12</b>
2.3 <b>Point Merge Principle .....</b>	<b>12</b>
2.4 <b>Differences and advantages of PMS with respect to conventional procedures .....</b>	<b>13</b>
2.5 <b>Point Merge System design .....</b>	<b>14</b>
2.5.1 Key Dimensions of the PMS .....	15
2.5.2 Symmetry and Angles of the Point Merge System .....	16
2.5.3 Vertical separation of the sequencing legs .....	17
2.5.4 Multi-system Point Merge .....	17
<b>CHAPTER 3. PERFORMANCE MODEL .....</b>	<b>19</b>
3.1 <b>Initial Segment .....</b>	<b>21</b>
3.2 <b>Sequencing Leg Segment .....</b>	<b>22</b>
3.3 <b>CDO Segment .....</b>	<b>23</b>
3.3.1 Speed schedules .....	23
3.3.2 Clean configuration part .....	25
3.3.3 Non-clean configuration part .....	25
<b>CHAPTER 4. POINT MERGE SYSTEM DESIGN .....</b>	<b>26</b>
4.1 <b>Requirements and Design Space .....</b>	<b>26</b>
4.2 <b>Routes .....</b>	<b>28</b>
4.2.1 Arrival routes .....	28
4.2.2 Final Approach .....	28
4.3 <b>Initial approach .....</b>	<b>29</b>
4.4 <b>PMS Conceptual Design .....</b>	<b>30</b>
<b>CHAPTER 5. MIXED INTEGER LINEAR PROGRAMMING FORMULATION .</b>	<b>33</b>
5.1 <b>Mixed Integer Linear Programming .....</b>	<b>33</b>
5.1.1 Constraint Position Shift .....	33
5.1.2 Rolling Horizon .....	34
5.2 <b>Sets and parameters .....</b>	<b>36</b>
5.3 <b>Decision variables .....</b>	<b>37</b>

<b>5.4 Objective function</b> .....	<b>38</b>
5.4.1 Minimize makespan .....	38
5.4.2 Minimize total fuel consumed .....	38
<b>5.5 Constraints</b> .....	<b>39</b>
5.5.1 Single Route .....	39
5.5.2 Initial Leg Time and Speed .....	39
5.5.3 Sequencing Leg Time and Speed .....	40
5.5.4 Continuous Descent Approach time and speed .....	42
5.5.5 Ordering Constraint .....	42
5.5.6 Separation .....	43
5.5.7 Total Transit Time .....	48
5.5.8 Fuel Consumption Constraint .....	48
 <b>CHAPTER 6. PERFORMANCE ANALYSIS</b> .....	 <b>49</b>
 <b>6.1 Graphic Outputs</b> .....	 <b>51</b>
6.1.1 Speed vs altitude .....	52
6.1.2 Altitude vs distance .....	54
6.1.3 Time vs distance .....	58
6.1.4 Time vs distance .....	59
 <b>CHAPTER 7. CONCLUSIONS</b> .....	 <b>63</b>
 <b>CHAPTER 8. BIBLIOGRAPHY</b> .....	 <b>65</b>



## Introduction

Since the start of aviation [1], there has been a continuous growth in air transport. This has resulted in the congestion of the current available airspace. In fact, one of the bottlenecks of future growth in the air transport industry is this congestion. That is one of the reasons for the need to optimize the available airspace and aim for a greater flight efficiency. Both Europe and the United States have started research studies to look for solutions to cope with the increasing air traffic such as SESAR and NextGen, respectively.

The optimization of the available airspace is achieved by improving Air Transport Management and by implementing new technological improvements in the Communication, Navigation and Surveillance (CNS) environment. This led to the introduction of the Performance Based Navigation (PBN) concept, which aims to improve the navigation.

Nowadays, the airport arrival procedures consist on Standard Terminal Arrival Routes (STARs), which are pre-defined routes consisting of different waypoints, in which there may be holdings to ensure a safe separation. These procedures end at the start of the instrumental approach procedure. The computer on board, which is the Flight Management System (FMS), is the responsible for generating the optimum descent path. In order to do that, it needs to know the remaining distance to the runway. However, during peak hours the Air Traffic Control (ATC) uses radar vectoring to sequence and space aircraft before landing, which makes the distance to the runway unknown.

The purpose of the STARs is to simplify clearance delivery procedures and to facilitate transition between the en-route and approach phases. Their drawback is that these procedures need a constant guidance from ATC, who indicate the pilots when to hold or which flight level they must fly in order to avoid conflicts with other flights. But when ATC is forced to use radar vectoring the workload increases, as a large amount of radio communication between the controller and the pilot is required to direct the aircraft to the right position. In addition, for both the controller and the pilot a loss of situational awareness arises due to complexity and difficulty to predict aircraft vertical profiles. This causes aircraft flying at lower altitudes and creating unnecessary noise, emissions and inefficient descents.

There has been a lot of research in this field in order to improve these arrival procedures and to improve the capacity and efficiency of the operations. Continuous Descent Operations (CDOs) work on that; they allow aircraft to follow an optimum flight path that delivers major environmental and economic benefits [1].

New air traffic managements (ATM) paradigms aim to efficiently implement 4D trajectories. Some strategies as 4D trajectories with fixed lateral route and open-loop vectoring as point merge and tromboning are being assessed.

The tromboning is a trombone shape RNAV procedure consisting in a set of parallel legs composed of multiple waypoints, in which ATC may give a shortcut (depending on the traffic) to the next leg reducing the total descent length. Works on this subject [2] propose a concept consisting of separating,

sequencing and merging traffic by negotiating required time of arrival (RTAs) and shortcuts between aircraft and ATC before starting the descent. Results from preliminary studies show that, for a given RTA, several shortcuts could be assigned such that the RTA fits into the feasible time window.

Furthermore, EUROCONTROL designed a special technique as a part of the PBN concept, which is called the Point Merge System (PMS). In PMS, aircraft fly sequencing legs at a constant altitude, until “direct to” instructions are given to a merge point, used for traffic integration. The PMS is designed to cope with high traffic loads without radar vectoring with the goal to reduce the workload of both the ATC and the pilots. It is also expected to improve the efficiency of the routes by restricting the flight level variations and minimizing the holding time. According to studies performed [5], aircraft can potentially save up to more than 100kg of fuel in the terminal area and reduce the mean controller task load and the number of instructions to pilots by 20% and 30% respectively. However, the environmental benefits of the PMS are limited to altitudes below the sequencing leg altitude, since the remaining distance is known with certainty only after the “direct to” instruction.

The PMS is already successfully implemented in the TMA at more than ten airports around the world, however no yet at Berlin-Schönefeld Airport.

The motivation of this project is to take profit of all these concepts and new procedures that are arising through the world and propose a new arrival design using the point merge system at Berlin-Schönefeld Airport. It is interesting to find out if the discussed advantages of the PMS could be applied to this airport.

A study of the potential benefits and drawbacks of the implementation of a new approach procedure in an existing TMA using a systemized method for merging arrival flows with closed loop instructions, denoted Point Merge, will be performed. The design will take into account important parameters such as the existing arrival and departures routes and the real traffic.

In this project a Point Merge System will be designed for the Berlin-Schönefeld Airport, precisely for the approach of runway 07L. The existing approach and departure routes will be taken into account and will remain untouched. The route will be designed fulfilling all the operational and safety requirements.

## CHAPTER 1. OPERATIONAL CONTEXT

### 1.1 Airspace and control phases

The procedures described in this project are concerned with the arrival phase of flights, typically starting when aircraft leave their cruise level in the en-route phase, having reached their Top of Descent (TOD), and ending when aircraft reach the FAF or are transferred to the Tower. This phase mainly relates to Terminal Airspace and includes the Terminal Maneuvering Area (TMA), and Approach control. Although it is a rather specific notion, an Extended Terminal Area (E-TMA) may also be introduced to handle high-density managed airspace dealing with traffic inbound to one or several major airport(s). E-TMA could be considered as a transition between en-route and TMA sectors, generally corresponding to delegated airspace from en-route and covering the control phase of flights that are already in descent, or about to start descent, leaving the en-Route network, but have not entered the TMA yet [1].

Consequently, for the purpose of this project, as depicted in figure 1.1 below, and although the TMA formally encompasses the approach, we will consider for arrivals in terminal airspace the succession of E-TMA, TMA, and inside TMA, the approach:

- E-TMA/TMA, including ACC terminal interface sector(s) and/or possibly TMA sector(s), typically between the TOD and the IAF.
- Approach airspace / Approach control phase, corresponding to Approach (APP) arrival sectors, typically between the IAF and the FAF or transfer to the Tower.

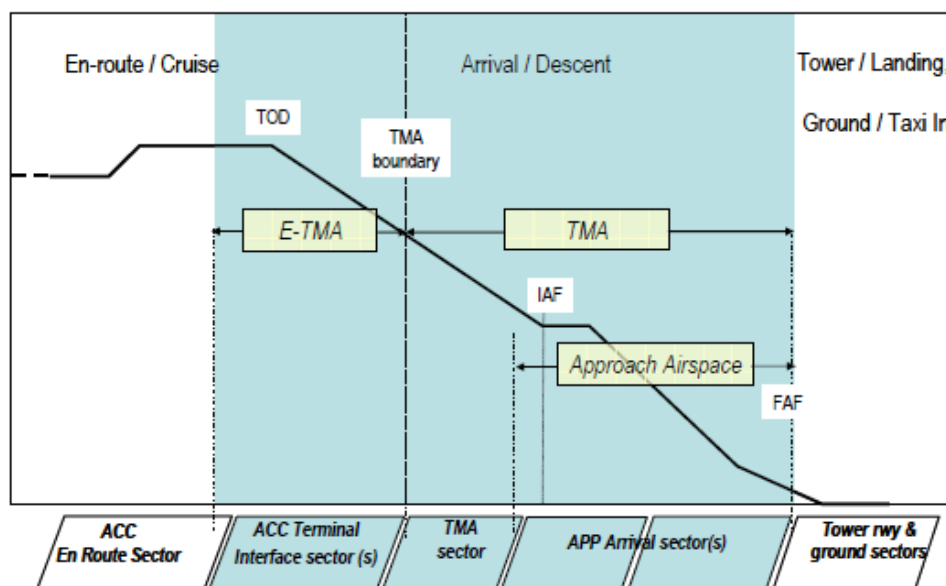


Figure 1.1: Control phases and sectors for the arrival phase of flight [1]

Note: in practice, depending on the local organization:

- TMA sector controllers, when TMA sectors exist, may actually be either co-located with ACC terminal sector controllers, i.e. within an ACC, or co-located with APP sector controllers.
- The IAF, and associated holding stacks when defined, may be within the area of responsibility of a TMA sector, or (as depicted above) of an APP sector.
- E-TMA, when defined/applicable, corresponds to “ACC Terminal Interface” sectors depicted above.

## 1.2 Air traffic control tasks

In terminal airspace, aircraft approaching one or more airport(s) from surrounding sectors typically follow a number of STARs providing the transition from En-Route structure, and are progressively merged into a single flow for each active landing runway.

In this context, the goal to enable a safe, expeditious and orderly flow of air traffic translates into three main arrival tasks for the controllers:

- Separate arrivals from other arrivals.
- Separate arrivals from departures.
- Integrate arrivals safely and efficiently into a landing sequence to each runway.

Air traffic control (ATC) tasks also include:

- Separate arrivals and departures from terrain/obstacles (subject to the operational context, according to the ICAO regulation governing responsibility for terrain clearance).
- Prevent unauthorized entry into segregated areas.

In E-TMA, ATC tasks include the following specific arrival tasks:

- Separate arrivals from over flights.
- Integrate arrivals safely and efficiently into intermediate sequence(s).

## 1.3 Integration of arrivals

### 1.3.1 Convergence versus spacing

This project is specifically concerned with the following ATC tasks:

- Integrate arrivals safely and efficiently into a landing sequence to each runway.
- Integrate arrivals safely and efficiently into intermediate sequence.

Formally, a “safe and efficient” arrival sequence refers to the provision of a throughput as close as possible to the available or required runway (or downstream airspace) capacity, while conforming to applicable separation

requirements. This in turn corresponds to two main objectives that may appear as contradictory and can be seen represented in figure 1.2:

- Ensure (progressive) convergence, ultimately towards the runway, in all dimensions (lateral, vertical and longitudinal).
- Ensure spacing (longitudinally) for metering purposes, or for separation (in at least one dimension: laterally, vertically, or longitudinally) ultimately towards the required runway separation.



**Figure 1.2: Convergence versus separation objectives [1]**

These objectives are realized through the achievement of both:

- An appropriate sequence order, driven by the need to optimize runway capacity usage.
- An appropriate inter-aircraft spacing, driven , again by the need to optimize runway capacity usage (maintaining a sufficient “pressure” to the runway regardless of the sequence order) and by the need to:
  - Ensure safe distances between flights tactically.
  - Anticipate, in so far as possible, on downstream capacity constraints.

### 1.3.2 Intermediate and final sequences

Schematically, the integration of arrival flows involves a progressive convergence along the lateral, vertical and longitudinal/time dimensions, ultimately to the runway. Due to this progressive nature, intermediate sequences must generally be built, and traffic flows synchronized in view of achieving the global sequence towards the runway. Therefore, the integration of arrivals may be broken down into the management of a succession of intermediate sequences to intermediate merging points, eventually leading to the final sequence of the runway.

Managing intermediate arrival sequences, typically in E-TMA/TMA sectors, aim at achieving the following operational objectives:

- Sequencing, ordering, of flights.
- Separation.
- Metering (e.g. towards an IAF, or a metering point before an IAF).

Managing the final landing sequence (typically in the Approach) involves the following objectives:

- Final sequencing, ordering, of flights.
- Separation towards the runway.

### 1.3.3 Phases in sequence management

The management of each sequence (be it intermediate or final) can also be described according to the following phases (see figure 1.3), each retaining all operational objectives depicted above (sequencing, separation and metering):

1. **Planning/Preparing** the sequence: landing runway allocation, sequence order and appropriate spacing.
2. **Building** the sequence: creation of order and appropriate inter-aircraft spacing.
3. **Maintaining** the sequence: maintenance of sequence order, and maintenance/refinement of inter-aircraft spacing.

Due to the fact that the planned sequence can evolve, there may be overlaps between these phases, as shown in the diagram below.

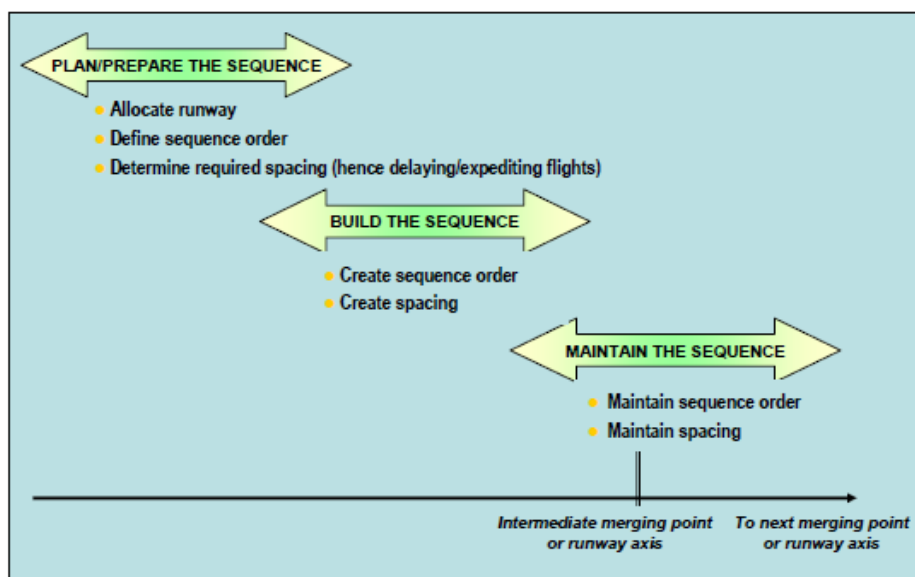


Figure 1.3: Phases in the management of the intermediate or final sequences [1].

### 1.3.4 Lateral path stretching or shortening

For the purpose of integration arrival flows, the building and maintenance of a sequence require the ability to expedite or delay aircraft in order to achieve longitudinal spacing. When traffic demand rises, and, or depending on traffic presentation, speed adjustments may not be sufficient and path shortening/path stretching may become necessary. It is therefore essential in dense terminal airspace, that any arrival integration technique provides enough flexibility to enable sufficient path stretching/shortening capability, to the extent of airspace capacity.

## 1.4 Conventional operating methods

The progressive merging of arrival flows into a runway sequence is usually performed in current day of operations through the use of open-loop vectoring when patch stretching/shortening is required. In the scenario of high traffic, air traffic controllers normally issue a vast number of heading, FL/Altitude and speed instructions. This method is highly flexible; however it results in high workload for both controllers and flight crews [11].

Additionally, it is not efficient for the flight crew or the operation of the aircraft (especially regarding vertical profiles): with open-loop vectors, flight crews' situation awareness is poor, and FMS cannot find the optimum descent trajectory as the distance to go is unknown. The use of open-loop vectors also causes inefficiencies in the ground system: ground-based tools involving trajectory prediction, such as conflict detection tools or AMAN, cannot be updated appropriately since the time when/location where aircraft will resume their normal navigation is not known. In case an AMAN is used, the sequence manager may not be fully aware of other controllers' intentions when they are vectoring aircraft.

In E-TMA/TMA sectors, where a route structure is generally defined, controllers give speed and/or heading/direct-to instructions as needed to separate and/or meter (pre-regulate) arrivals towards TMA entry points or IAFs.

In the Approach phase, generally after passing the IAF, in the absence of a route structure, controllers further vector the aircraft to fine tune the arrival sequence and integrate traffic flows from different IAFs to the runway axis. In dense and/or complex environments, controllers tend to follow a strategy giving themselves more time and margins to implement and fine tuning the sequence. This usually results in aircraft flying at low altitudes and at slow speed. Furthermore, the lack of a 2D structure often leads to a tactical management of conflicts with other flows, inducing intermediate levels offs.

### 1.4.1 Advanced procedures and tools

Nowadays, arrival procedures have evolved into more accurate ones allowing more aircraft operations in the same airspace. Precision Area Navigation (P-RNAV) arrival procedures have been implemented in the vicinity of some European airports, with the goal of improving workload, airspace capacity, predictability, efficiency and/or environment-related benefits. These procedures have been designed with the aim of replacing open-loop vectors in Approach for arrivals, and allowing revisiting associated working methods. However, it shall be remarked that benefits in all of these areas cannot usually be achieved through a single procedure, and trade-offs may have to be considered, or put focus on certain Key Performance Area (KPA), according to local constraints [7].

For instance, RNAV procedures providing the most direct routes have been defined in Stockholm to support flight-efficient descents (Continuous Descent

Operations). However these procedures are not meant to increase capacity and are generally used only in low traffic density scenarios.

On the other hand, in order to integrate arrival flows in dense traffic situations, trombone-shaped RNAV transitions have been in use in Munich or Frankfurt for a significant period of time now. These procedures roughly replicate typical vectoring patterns. They include a set of regularly spaced waypoints defined in the downwind and final approach segments, aiming at supporting path stretching/shortening through route changes, while normally keeping the aircraft on lateral navigation.

This design has proved to be an effective method of sequencing the traffic flows to the runways. It results in a significant path stretching capability to the extent of available airspace. However, such RNAV procedures are normally fully applied only in cases of low to medium traffic loads. The main disadvantage of RNAV procedures is that they reduce the flexibility that radar vectoring allows to the controller and experience has shown that, without the help of a very advanced arrival manager, controllers tend to revert to radar vectoring during the peak periods. Also, Precision Area Navigation (P-RNAV) applications in the terminal area have not realized all the anticipated benefits of reduced cost, increased capacity and improved environment. P-RNAV procedures can be integrated with conventional procedures and can bring operational, financial and environmental benefits in light to medium traffic loads. However, at high traffic loads, the controllers inevitably revert to radar vectoring in order to maximize capacity.

The reasons for these limitations are that:

- The discontinuity of lateral alterations of trajectories through pre-defined tactical waypoints does not enable controllers to easily ‘fine-tune’ spacing between successive aircraft. This is especially the case during periods of high traffic load, where it is a common practice for controllers to use radar vectoring techniques between downwind and final to ensure runway throughput is optimized by reducing spacing between aircraft to the extent possible.
- Route changes with a large set of available waypoints may require lengthy manipulation in the cockpit possibly resulting in a long reaction time when a route change is instructed, and risk of confusion or errors.

Finally, whilst ‘trombone’ shaped RNAV transitions may simultaneously offer a large path stretching capability and allow maintaining runway pressure and offer high flexibility in ‘filling the gaps’ in the sequence (i.e. in case of a go-around), such flexibility requires anticipating on path shortening, hence early descents, and non-optimal vertical profiles. Again, the notion of a trade-off between some KPAs, as opposed to maximum benefits in every KPAs, has to be considered.

## 1.5 Continuous descend operations

Continuous Descend Operations (CDOs) [11] are an aircraft operating technique aided by appropriate airspace procedure design and appropriate Air Traffic Control clearances enabling the execution of a flight profile optimized to the operating capability of the aircraft. CDOs allow aircraft to perform a flexible and optimum flight path that delivers major economic and environmental benefits, reduced fuel burn, gaseous emissions, noise and fuel costs and without any adverse effect on safety. Figure 1.4 compares a CDO with a conventional descent.

CDOs allow arriving aircraft to descend continuously, to the greatest extent possible. Aircraft can employ minimum engine thrust, ideally in a low drag configuration, prior to the final approach fix. This technique results in the aircraft flying more time at more fuel-efficient higher cruising levels, hence significantly reducing fuel burn and lowering emissions and fuel costs. The optimum vertical profile takes the form of a continuously descending path, with a minimum of level flight segments only as needed to decelerate and configure the aircraft or to establish on a landing guidance system such as the ILS.

The optimum vertical path angle will vary depending on the type of aircraft, its actual weight, the wind, air temperature, atmospheric pressure, icing conditions and other dynamic considerations. A CDO can be flown with or without the support of a computer-generated vertical flight path, given by the flight management system (FMS), and with or without a fixed lateral path. However, the maximum benefit for an individual flight is achieved by keeping the aircraft as high as possible until it reaches the optimum descent point which is most readily determined by the onboard FMS.

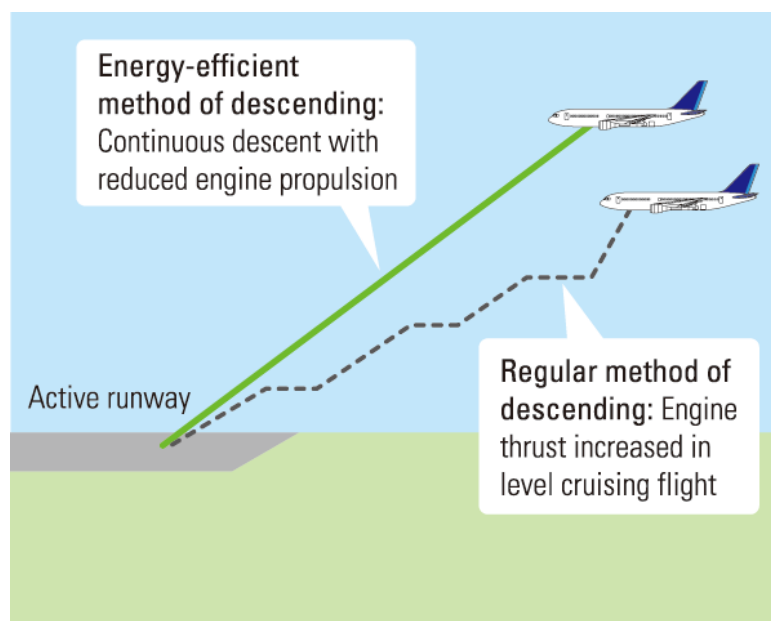


Figure 1.4: Vertical path angle [18]

Air traffic controllers are required to provide safe and efficient management of arriving aircraft. However, the term “efficiency” can mean different targets to different stakeholders and may vary depending on traffic density levels, aircraft mix or weather. To achieve overall arrival and departure efficiency, a balance should be struck between expediting traffic, meeting airport capacity, and reducing flight times, flight distances, fuel burn, emissions and noise within the overall requirement for safe operations. Environmental impact is a significant issue for aviation in general and should be considered both when designing airspace and instrument flight procedures, and when managing aircraft operations. Specifically, techniques that enable a fuel-efficient (minimum thrust) optimum descent and approach should be used wherever and whenever possible. The total energy of the aircraft at high altitude can be used most efficiently during descent with minimum thrust and drag. The pilot should however have the maximum flexibility to manage the aircraft’s speed and rate of descent.

Deployment of CDOs throughout Europe will be beneficial to all European ATM system stakeholders [1] and will help the network to address the environmental challenges it faces. The results of EUROCONTROL studies have shown that on average, the benefit of flying CDOs would result in fuel savings up to 350,000 tons of fuel or more than 150 million euros. In addition, the application of CDOs could minimize the noise by 1dB to 5dB compared to a non CDO operation.

CDOs offers the following advantages:

- a) More efficient use of airspace and arrival route placement;
- b) More consistent flight paths and stabilized approach paths;
- c) Reduction in both pilot and controller workload;
- d) Reduction in the number of required radio transmissions;
- e) Cost savings and environmental benefits through reduced fuel burn;
- f) Authorization of operations where noise limitations would otherwise result in operations being restricted.

## CHAPTER 2. THE POINT MERGE SYSTEM

### 2.1 Point Merge System History

The continuing growth of aviation increases demands on airspace capacity, thus emphasizing the need for optimum utilization of available airspace. Improved operational efficiency derived from the application of area navigation techniques has resulted in the development of navigation applications in various regions worldwide and for all phases of flight. These applications could potentially be expanded to provide guidance for ground movement operations.

One of the first methods of aerial navigation of the modern days was performed by ground-based navigations aids such as Distance Measuring Equipment (DME), VHF Omni-directional Range (VOR) and Non Directional Beacon (NDB). Using this ground aids the aircraft flew directly towards the navigation aid and then selected another one to follow a predefined path in the Flight Management System (FMS).

After, the Area Navigation (RNAV) was developed and introduced. RNAV is a method of instrumental flight rules (IFR) navigation that allows an aircraft to choose any course within a network of navigation beacons, rather than navigate directly to and from beacons. The RNAV system is primary based on ground-based navigation aids such as two or more DMEs or, less accurately, a VOR and DME. This made it possible for the aircraft to deviate from the constraint ground-based conventional route and enable point-to-point navigation along a set of waypoints. This method can conserve flight distance, reduce congestion, and allow flights into airports without beacons. Area navigation used to be called “random navigation”, hence the acronym RNAV.

RNAV was developed in the United States in the 1960s, and the first such routes were published in the 1970s. In January 1983, the Federal Aviation Administration revoked all RNAV routes in the contiguous United States due to findings that aircraft were using inertial navigation systems rather than the ground-based beacons, and so cost–benefit analysis was not in favor of maintaining the RNAV routes system. [2] RNAV was reintroduced after the large-scale introduction of satellite navigation.

Two types of RNAV exist, namely Basic Area Navigation (B-RNAV) and Precision Area Navigation (P-RNAV). The difference is the accuracy of the RNAV. B-RNAV has a navigation performance equal to or better than a track keeping accuracy of  $\pm 5$  Nautical Miles (NM) for 95% of the flight time and was the standard from 1998. As the demand of RNAV operations increased there was a need for an improvement in the accuracy and P-RNAV was introduced in 2006. P-RNAV has an accuracy of  $\pm 1$  NM for 95% of the flight time. This makes P-RNAV suitable to be used in the TMA of an airport which can provide Air Traffic Control (ATC) interesting possibilities for the control of approaching aircraft. Instead of one arrival track, several tracks can be added alongside this one track. This gives the ATC more options for sequencing aircraft. In this way ATC does not have to vector each aircraft individually, but can send them on

different tracks instead resulting in a reduced workload and decreases the risk of ATC error. However, there are two disadvantages: first, if there are many optional routes in the navigational charts, the readability will decrease and, second, during peak hours the ATC uses heading instructions for merging aircraft flows in the TMA in order to maximize capacity, an open-loop system. Since the introduction of Area Navigation (RNAV), EUROCONTROL is proposing new options for merging traffic in the TMA. To provide a solution for these disadvantages without changes in the phraseology and FMS modifications to speed up the implementation process, EUROCONTROL started to investigate a special method for merging the flows in the TMA denoted as the PMS. The following goals are defined for the PMS: maintain the possibility of guidance by the FMS and make CDA possible, even under peak traffic loads.

## 2.2 Current applications of the point merge concept

In figure 2.1 it can be seen how Point Merge has been gradually implemented in different airports around the world since it was developed by the EUROCONTROL Experimental Centre in 2006 [3].

Point Merge is now operational in Oslo (2011) and three Norwegian regional airports (2014), Dublin (2012), Seoul (2012), Paris ACC (2013), Kuala Lumpur (2014), Lagos (2014), Canary Islands (2014), Hannover (2014), Leipzig (2015) and London City and Biggin Hill (2016).

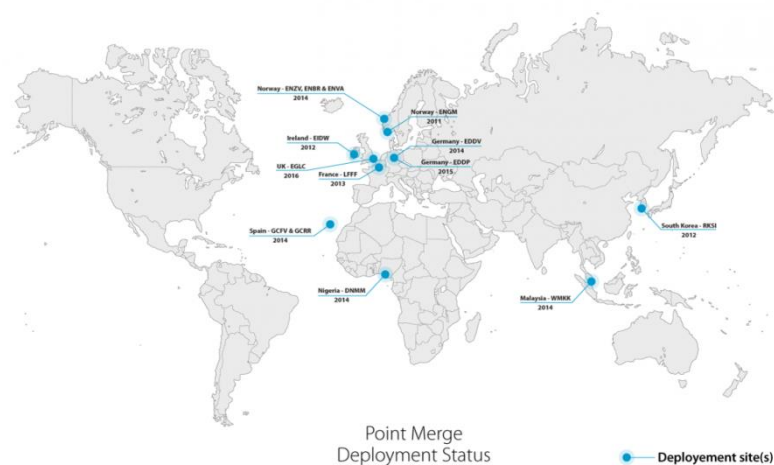
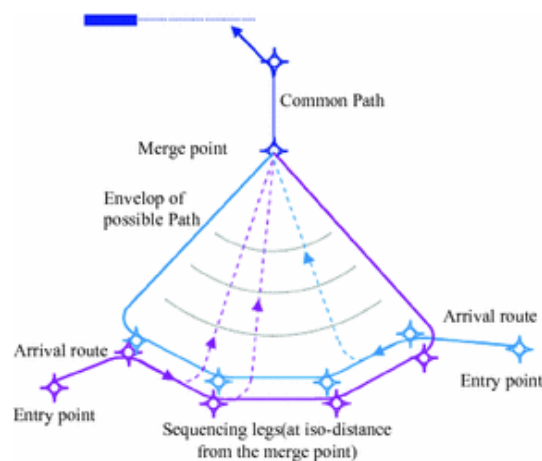


Figure 2.1: Point Merge deployment status [3]

## 2.3 Point Merge Principle

Point Merge is an innovative procedure developed in 2006 by the EUROCONTROL Experimental Centre (EEC) to merge arrival flows of aircraft. Point Merge aims at improving and harmonizing arrival operations with existing technology. It enables continuous descent approaches even under high traffic loads, with a potential average fuel saving of 100kg per aircraft in the terminal area.

[1] The Point Merge is supported by P-RNAV systems and allows sequencing efficiently the traffic on runway final approach, making possible the continuous descent approach, even with high traffic circumstances. A point merge sketch can be seen in figure 2.2. The arrival routes which work with the Point Merge system have a convergent geometry that allows the path stretching or shortening, and comprise a merge point, where traffic is integrated into the runway final approach in a single flight path, and sequencing legs, which are predefined by waypoints and should be isodistant and equidistant from the merge point and shall be separated from each other on lateral or vertical level. The sequencing legs can be seen as an arc on a circle with a distance to the merge point equal to the radius of the circle.



**Figure 2.2: Point Merge sketch [1]**

The aim of the PMS is to integrate the inbound arrival flows and comprises of two phases: first, create spacing and, second, maintain spacing. This is achieved by letting the aircraft fly over the sequencing legs until enough spacing is reached then the ATC instructs a “direct-to” command to the merge point. The aircraft will immediately turn to the merge point and fly directly to it. In the approach to the merge point, the controllers must ensure that flights are properly separated and if necessary give speed control instructions to avoid the violation of these separations.

To simplify the separation between aircraft and to sequencing them, RNAV STAR's that allow an effective transition from en-route phase to the runway approaching phase of the flight, sequencing the traffic into a single stream to the runway, are employed. The terminal airspace controllers must ensure separation between arrivals/arrivals and arrivals/departures, and integrate the flights on the runway landing sequence in a safe and efficient way.

## **2.4 Differences and advantages of PMS with respect to conventional procedures**

The PMS route structure is based on a wedge shape with the aim of converging traffic to a single point. The advantages with respect to this shape are:

- A more intuitive and clearer route structure. The PMS has a predefined horizontal and vertical envelop due to the wedge shape pointed to the

merge point which results in an easier deconfliction of aircraft compared to vectoring aircraft.

Current procedures enclose sequencing, metering and separation aspects; however, PMS separates this into sequencing and spacing. Sequencing is the order in which the “direct-to” command is given to aircraft in the PMS and spacing relates to the interval between these commands. PMS involves a closed loop intervention keeping aircraft on lateral navigation even in dense airspace scenarios, requiring fewer tactical interventions if compared with conventional operations. However, a closed-loop intervention lead to less flexibility for the ATC.

The two main objectives of ATC on a tactical level are convergence in all dimensions and separation in at least one dimension. Convergence is obtained when the aircraft directs to the merge point. The advantage is that convergence in lateral and vertical plane only requires one instruction each; direct-to and descent, respectively. Separation is obtained by path stretching on the sequencing leg, requiring only one intervention, delaying the direct-to command. The workload of the ATC is highly reduced and permits a more efficient handling of the incoming traffic without losing safety.

Regarding the performance areas, the following advantages are identified:

- The main advantage of the PMS is the capability of using a CDA starting at the sequence leg until the final point of the system. This, compared to a step down approach eliminates level segments to keep aircraft at higher altitudes and minimizes the need of additional thrust during descent.
- The benefits of CDA are noise reduction, decrease in noise contour areas, reduction of emissions and fuel saving.

## 2.5 Point Merge System design

The PMS shown in figure 2.3 consists of one system with two arrival flows. However, the design can be adjusted to satisfy any airport situation. This section discusses the key dimensions, the angles and the vertical separation of the PMS. Then, multi-system options are described.

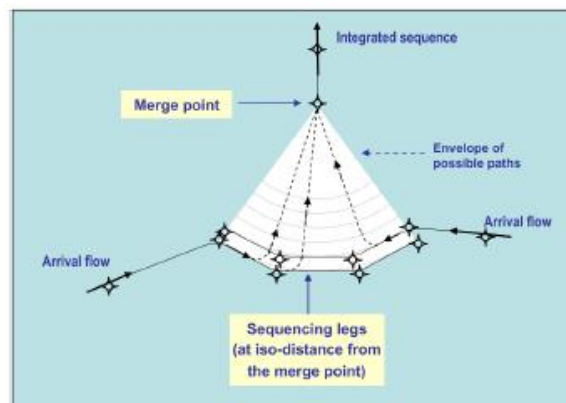


Figure 2.3: Example of the PMS with two inbound flows [1]

## 2.5.1 Key Dimensions of the PMS

The route structure of the PMS is shown in figure 2.4. The key dimensions of the PMS that can vary are:

- Length of the sequencing legs: An increase in the length of the sequencing legs can absorb delay, but this will make the PMS more sensitive to wind and will cover a larger area in the TMA.
- Distance between the sequencing legs and the merge point: Increasing the distance from the sequencing legs to the merge point will result in a better spacing ability and applicability of speed control. Additionally, the sequence is more predictable as it is made earlier. Despite that, this can make the resequencing of an aircraft during a missed approach more difficult.
- Height of the sequencing legs: If the height of the sequencing legs is increased, the environmental impact decreases and the efficiency of the flight increases. Furthermore, if combined with the stretching of the length to the merge point, the CDA can be started from a higher altitude. The downside of increasing the height of the sequencing legs is that the aircraft need to increase speed at higher altitudes which decreases the delay absorption.

Regardless of the above, it shall be remarked that the size of a Point Merge is expected to be limited by the following constraints:

- The size of the airspace available including the environmental constraints.
- The fact that the procedure shall be designed so the requirements of CDA are fulfilled for a mix of different aircraft types and performances.
- The number of entry points, the runway(s) in use and the complexity of the arrival and departure routes.
- Airspace sectorisation and boundaries: a Point Merge system that would extend across several sectors would obviously raise ATC operational issues.

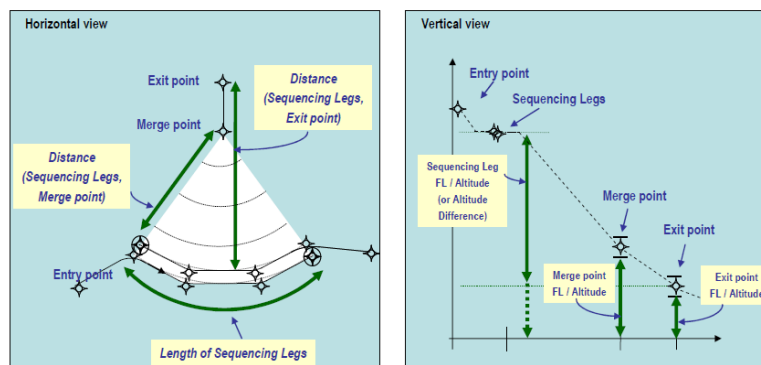


Figure 2.4: Point Merge horizontal and vertical view [1]

## 2.5.2 Symmetry and Angles of the Point Merge System

It is recommended, as a general principle, to ensure symmetry in the design of a Point Merge route structure, be it for single or combined Point Merge systems, in order to:

- Keep the operating method as simple and intuitive to apply as possible.
- Ensure better predictability of trajectories flown.

This symmetry principle applies in particular to distances (equidistance property) and angles (as detailed below).

In addition to the lengths, the angles in the design of the PMS can be varied to achieve the right dimension. The following angles can be defined in a Point Merge system (Figure 2.5):

- The track angle change at the first waypoint on the sequencing leg ( $\alpha$ ), and in case of segmented legs, subsequent track angle changes at successive waypoints on a sequencing leg ( $\alpha', \alpha'' \dots$ ).
- The track angle change corresponding to the direct-to instruction towards the merge point ( $\beta$ ).
- The angle formed by the envelope of possible routes to the merge point ( $\delta$ ).
- The track angle change at the merge point ( $\gamma$ ) to the exit point.

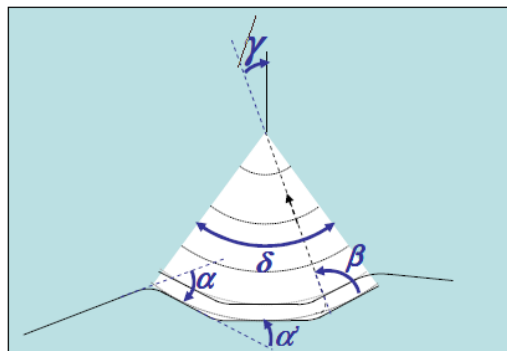


**Figure 2.5: Point Merge angles [1]**

As an illustration, iso-distant lines are shown in figure 2.5. However, these lines are not equidistant as the distance to the merge point is different for each iso-distant line. Ideally, the sequencing legs should be both iso-distant from the merge point and equidistant from the merge point meaning both sequencing legs are at an equal distance from the merge point. These two properties cause better predictability of the trajectories flown.

In order to respect the symmetry guidelines, the track angle at each waypoint needs to be constant. For the same reason angle  $\beta$  is almost constant at every point on the sequencing leg and approximately equal to  $90^\circ$ . If angle  $\delta$  is increased the sequencing leg length is also increased and vice versa. In the worst-case scenario, angle  $\delta$  is  $180^\circ$  which means that if two aircraft coming from opposing entry points and both take the shortest path to the merge point, both aircraft will fly a head-on course. This causes less flexibility in case of

issues and errors. As a baseline angle  $\delta$  is chosen in such a way that the sequencing leg is at least 20 nautical miles.

As a general rule for the design of a P-RNAV procedure,  $\alpha$  ( $\alpha'$ ,  $\alpha''$ ...) and  $\gamma$  shall be smaller than  $120^\circ$ , and as these angles correspond to fly-by transitions, they should be smaller than  $90^\circ$ . As already stated before, track angle changes at waypoints, along with the length of segments are key factors in the procedure design. Furthermore, large track angles changes at waypoints may increase the sensitivity to heterogeneous aircraft turn performances.

### 2.5.3 Vertical separation of the sequencing legs

By symmetrical design it is desired to have the sequencing legs as close as possible (at equidistance). This is favorable as the aircraft have to reach the same merge point and to keep the PMS possible for every class of aircraft.

As a general rule, differences in levels/altitudes used along the sequencing legs shall not be too large, this is due to the need to keep aircraft at compatible speed for sequence building/maintenance, and in view of their descent for reaching the same altitude at the merge point while ensuring longitudinal separation.

Parallel sequencing legs shall on the other hand be vertically separated each assigned with a different published level/altitude (i.e. at least 1000ft apart), using appropriate vertical restrictions. Consequently, a trade-off has to be found between the two requirements.

Although it may not seem natural, a Point Merge system shall generally be designed with the inner sequencing leg at the highest FL/altitude. The main reason for this is that there would be a reduced risk of separation infringement in case an aircraft unexpectedly descends just after being instructed to turn direct-to the merge point.

### 2.5.4 Multi-system Point Merge

The system shown in figure 2.3 concerns a single PMS with two arrival flows. However, depending on the number of inbound flows, it may be necessary to include more than two sequencing legs in the Point Merge design. Figure 2.6 below gives an example with three parallel legs in a single Point Merge system.

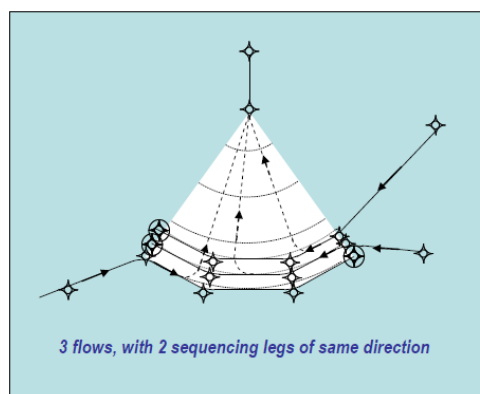


Figure 2.6: Point Merge of three parallel legs [1]

However, with three or more parallel sequencing legs, the decision time to instruct the direct-to turn towards the merge point may be significantly reduced if the leading aircraft is on the inner leg and the trailing aircraft is on the outer leg.

Furthermore, such configurations would require a large number of levels to be used in total, a larger distance between the legs and the merge point to allow for descent, and possibly a smaller distance between the sequencing legs to ensure the equidistance requirement is adhered to. Also with more than two levels used by the sequencing legs in a single Point Merge system, the availability of spare levels may become an issue.

Finally, note that in order to deal with configurations involving more than two or three inbound flows, another solution may be to combine Point Merge systems.

For example, in figure 2.7 two different options are shown for an airport with four arrival routes. First option is a single PMS containing four sequencing legs. However, due to the constraint of at least 1,000ft of vertical separation between the sequencing legs, the difference between the highest and lowest sequencing leg is 4,000ft which influences the CDA performance. Additionally, the aircraft come from different sectors, some of them requiring additional travel distance from the Initial Approach Fix to the entry point of the PMS. To overcome these issues, two identical PMSs can be created both with two sequencing legs merging at one point. Note in the figure below the offset between the merge points of the multi system which reduces the risk of a head-on encounter.

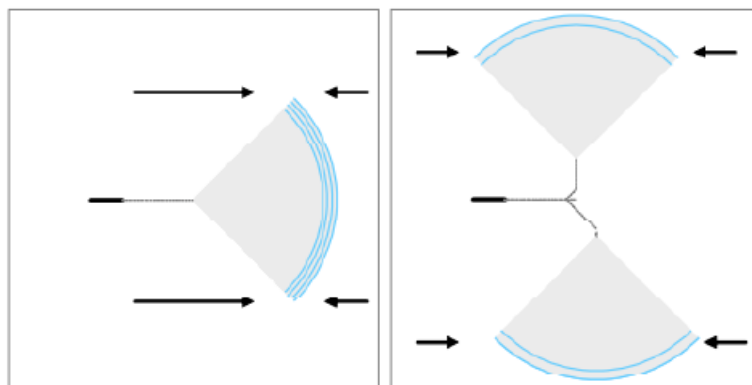


**Figure 2.7: Two possible design options for a PMS [1]**

## CHAPTER 3. PERFORMANCE MODEL

In this section the performance calculations of the aircraft inside the PMS will be discussed. The calculations simulate the limits [4] [10] and performance of the aircraft, serving as inputs for the scheduling model. BADA will be used in this section to simulate the performance of the different aircraft inside the PMS. BADA (Base of Aircraft Data) is an Aircraft Performance Model (APM) developed and maintained by EUROCONTROL, with the active cooperation of aircraft manufacturers and operating airlines.

BADA is designed for simulation and prediction of aircraft trajectories for purposes of ATM research and operations. Aircraft performance parameters and trajectories can be calculated using information and data contained in BADA. The BADA is not a software itself, however, it comprises the model specifications and the aircraft datasets comprising the aircraft specific coefficients.

BADA's Aircraft Performance Model is based on the Total Energy Model (figure 3.1), which equates the rate of work done by forces acting on the aircraft with the rate of increase in potential and kinetic energy. It can be considered as a reduced point-mass model.

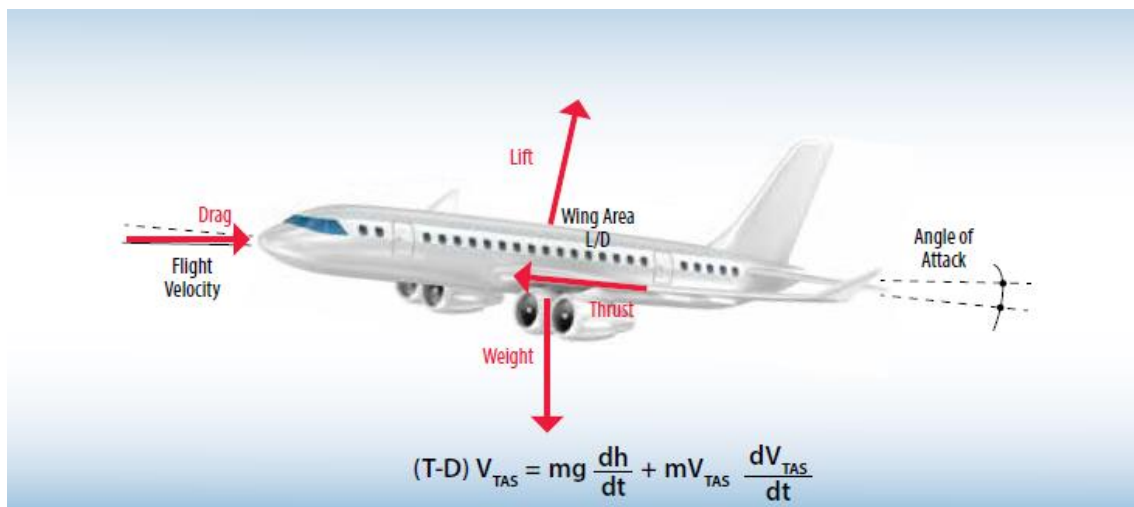


**Figure 3.1: BADA's APM model [10]**

The model is shown in figure 3.1. Assuming that the angle between the thrust vector and the velocity vector is small and no wind exists; the equation for the Total Energy Model is expressed as in equation 3.1.

$$(T - D) \cdot V_{TAS} = mg \frac{dh}{dt} + m V_{TAS} \frac{dV_{TAS}}{dt} \quad (3.1)$$

As shown in the previous figure four forces can be observed that act on the aircraft; Lift (L), Weight (W), Thrust (T) and Drag (D). Depending on these forces acceleration in the horizontal or in the vertical plan is obtained.

As previously discussed, in this research, contrary to the currently existing scheduling models, speed changes are allowed as an additional way to ensure the separation requirements. In order to reduce the communication between the pilots and the ATC to a minimum this speed changes are only allowed at the IAF and at the entry point of the PMS. Having said that, the PMS is split into three segments in every of which different performance calculations will be required. These segments are shown in figure 3.2.

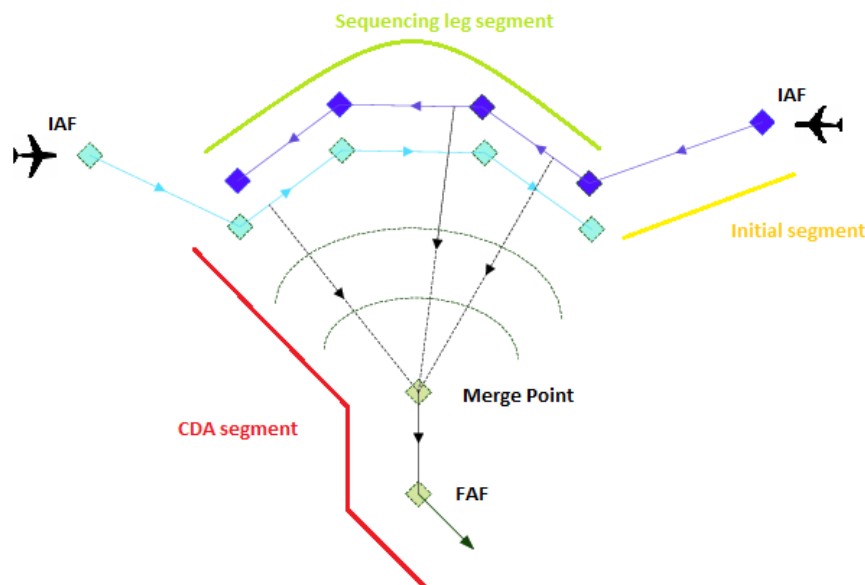


**Figure 3.2: Point Merge segments**

1. **Initial segment:** This segment starts at the IAF and ends at the entry point of the PMS. This segment has a fixed length and it is assumed to be level.
2. **Sequencing leg segment:** This segment comprises between the entry point of the PMS and the turn point of the aircraft (the point the aircraft receives the direct-to instruction). This segment's length is not constant due to the fact that the aircraft can turn at any time while they are on the sequencing leg. The altitude of this segment is also level.
3. **CDO segment:** This is the last segment that starts at the turn point and ends at the FAF. In this segment the aircraft flies performing a CDO towards the FAF. The length of this segment is fixed given the design of the PMS.

Next, the Total Energy Model is derived to achieve the performance required for each segment. First, the initial segment performance calculations are explained;

second the sequencing leg segment performance calculations are discussed, and last, the calculations for the CDO segment are explained.

Note that the mass of the aircraft is assumed to be constant from the beginning of the initial segment to the end of the CDO segment. The initial masses selected in this project are the average masses of each aircraft type found in the aircraft datasets of BADA.

### 3.1 Initial Segment

When the aircraft starts the initial segment, it is permitted to change the separation by speed control. Consequently, the fuel flow of the aircraft varies due to the change in speed, and each aircraft type has a different fuel flow. To obtain the fuel flow a feasible velocity range has to be calculated.

In our project we have two IAFs which mean we have two initial different initial segments. As seen in the design, one sequencing leg is at a height of 10,000ft and the other sequencing leg is at a height of 9,000ft and as previously discussed the initial segments are level and at the same altitude as the sequencing leg. Moreover, it is assumed that the selected velocity remains constant through the whole segment. Using BADA, we obtain that a level flight with constant velocity is a cruise flight. By setting the thrust equal to the drag we obtain the equation that models a cruise flight.

$$T = D \quad (3.2)$$

Given the fact that the change in height and speed over time is zero we obtain equation 3.2 from equation 3.1. The drag of each aircraft can be calculated using BADA and then the thrust can be computed. To compute the drag acting on each aircraft equation 3.3 is used. Using the coefficients obtained in BADA the drag coefficient is computed. In the initial segment the aircraft is assumed to be still in cruise configuration, also known as “clean” configuration. In cruise configuration there are not any lift devices or landing gear deployed. To simplify things, the bank angle correction in the lift coefficient is assumed to be zero. With these, the lift coefficient is computed using equation 3.4.

$$D = \frac{1}{2} C_D \rho V_{TAS}^2 S \quad (3.3)$$

$$C_L = \frac{2mg_0}{\rho V_{TAS}^2 S \cos\phi} \quad (3.4)$$

Analyzing equation 3.3, we know that given the fact that in the initial segment the height is constant so the air density is constant. Also, as previously stated, the aircraft is in cruise configuration which means that the wing surface of the aircraft is constant. Finally, the true airspeed is the only variable in the equation. That means that when a true airspeed is chosen, the needed amount of thrust is obtained. Once the thrust is obtained, the thrust coefficient can be calculated, and combining the thrust coefficient with the coefficients obtained in BADA, the fuel flow per second can be computed. In figure 3.3, the fuel flow per second of a Boeing 737-800 aircraft is represented for a range of true airspeeds.

The fuel flow we are looking for is the fuel flow per nautical mile, because by design, although the time inside the initial segment is variable, the distance is fixed. Therefore, dividing the fuel flow for each aircraft's true airspeed the fuel flow per nautical mile is obtained and with it we can calculate the total fuel consumption of this segment.

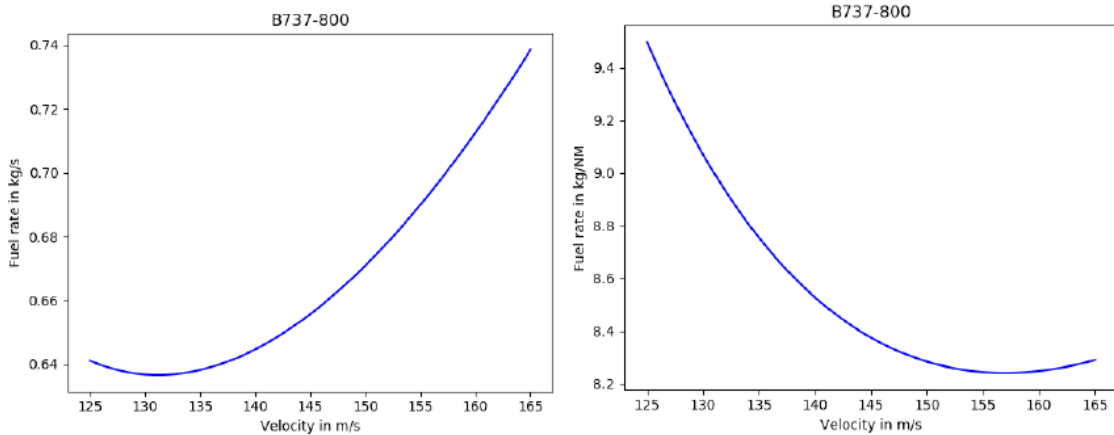


**Figure 3.3: Fuel flow per second and per nautical mile [4]**

In figure 3.3, the fuel flow per nautical mile for a range of true airspeeds can be seen, in this case the Boeing 737-800 is again taken as example. In order to continue, the range of feasible velocities has to be found. Defined by regulations, the maximum true airspeed below 10,000ft is 250 knots calibrated airspeed. To calculate the true airspeed using the calibrated airspeed equation 3.5 is used.

$$V_{TAS} = \left[ \frac{2p}{\mu\rho} \left( \left( 1 + \frac{p_0}{p} \left[ \left( 1 + \frac{\mu\rho_0}{2p_0} V_{CAS}^2 \right)^{\frac{1}{\mu}} - 1 \right] \right)^{\mu} - 1 \right) \right]^{\frac{1}{2}} \quad (3.5)$$

Notice that the true airspeed depends on the altitude of the aircraft. As a result, the maximum true airspeed at 10.000ft is higher than the maximum true airspeed at 9.000ft.

Now, the minimum true airspeed. Usually, the minimum true airspeed in cruise is not lower than the maximum endurance speed. That is the airspeed where the fuel flow in kg/s is minimal.

### 3.2 Sequencing Leg Segment

The sequencing leg segment starts just after the initial segment. In this segment the length can vary from one aircraft to another due to the fact that the length of this segment depends on the turn point of the aircraft. The length of this segment can vary from zero, when no path stretching is required, and the maximum length of the segment which is the total length of the sequencing leg. The scheduling model requires as input the fuel flow and the feasible speed range of this segment. Like the initial segment, the aircraft performances in this segment can be modelled as cruise flight. Therefore, the calculations of velocity

speed range and fuel flow are obtained using the same calculations as in the initial segment.

### 3.3 CDO Segment

The continuous descent segment starts once the aircraft has arrived at the turn-point on the sequencing leg. This is the beginning where it will start descending towards the runway. The flight time and fuel consumption of the entire CDO profile for each aircraft type is required for the scheduling model.

As explained in the beginning of the project and according to ICAO [11], a CDO is a technique in which the aircraft continuously descends, to the greatest possible extent, by employing minimum engine thrust, ideally in a low drag configuration, prior to the FAF.

In BADA, two independent control inputs can be employed to reach a descent: the elevator and the throttle. By using these control inputs three variables can be controlled: thrust, rate of descent and speed. And by controlling the thrust and speed a rate of descent is obtained. By controlling the rate of descent and thrust a speed is obtained, and by controlling the rate of descent and speed a required thrust is obtained.

Two control inputs have to be chosen. The CDO is composed by two parts. The first part, called clean configuration, and the second part, when the approach/landing configuration is active, called also the non-clean configuration. Normally, aircraft descend with a constant calibrated airspeed. Therefore, BADA has standard defined airline procedures where the speed schedule of descent is defined, making the airspeed the first control input for both parts. The, for each part a different second control input will be needed:

- Clean configuration part: As defined by ICAO, in the CDO the thrust for the clean configuration segment is the minimum engine thrust. In BADA, minimum engine thrust is defined as idle thrust and it can be calculated using BADA. Therefore, for the clean configuration part the thrust will be a controlled input.
- Non-clean configuration part: Once the configuration is switched to a non-clean configuration, a constant rate of descent has to be flown, requiring the thrust to be increased to maintain the airspeed in the speed schedule. Therefore, for this part the controlled input will be the rate of descent.

#### 3.3.1 Speed schedules

BADA defines standard airline procedures. The descent speed schedules are included in this procedure and they are shown in table 3.1. The table is divided in range of heights and for each one a descent CAS is defined. The standard descent CAS depends on each aircraft and is included in the BADA database.

**Table 3.1.** Descent speed schedules

Height (ft)	CAS (knots)
From 0 to 999	$C_{Vmin} * (V_{stall})_{LD} + Vd_{DES,1}$
From 1,000 to 1,499	$C_{Vmin} * (V_{stall})_{LD} + Vd_{DES,2}$
From 1,500 to 1,999	$C_{Vmin} * (V_{stall})_{LD} + Vd_{DES,3}$
From 2,000 to 2,999	$C_{Vmin} * (V_{stall})_{LD} + Vd_{DES,4}$
From 3,000 to 5,999	$\min(V_{des,1}, 220)$
From 6,000 to 9,999	$\min(V_{des,1}, 250)$
From 10,000 to Mach transition altitude	$V_{des,2}$

Below an altitude of 3,000ft, the descent CAS is a sum of the landing stall speed ( $(V_{stall})_{LD}$ ) multiplied by the minimum speed coefficient ( $C_{Vmin}$ ) and a descent increment speed ( $Vd_{DES}$ ). Between an altitude of 3,000ft and 6,000ft, the CAS descent is the standard descent CAS ( $V_{des,1}$ ) or 220knots, whichever is lower. For altitudes between 6,000ft and 10,000ft, either the standard CAS ( $V_{des,1}$ ) is used, or the maximum velocity of 250knots CAS is maintained, whichever speed is lower. For altitudes from 10,000ft to the Mach transition altitude the standard CAS ( $V_{des,2}$ ) is maintained.

The minimum speed coefficient is a constant of 1.23, and the descent speed increments depend on the height and are shown in table 3.2.

**Table 3.2.** Descent speed increments

Height (ft)	Variable Name	CAS increment (knots)
From 0 to 999	$Vd_{DES,1}$	5
From 1,000 to 1,499	$Vd_{DES,2}$	10
From 1,500 to 1,999	$Vd_{DES,3}$	20
From 2,000 to 2,999	$Vd_{DES,4}$	50

Finally, the stall speed has to be computed. Equation 3.4 can be adjusted to compute the stall speed shown in equation 3.6. From it we can see that instead of the  $C_L$ , the maximum lift coefficient ( $C_{Lmax}$ ) is used. The stall speed is dependent on the aircraft configuration and type.

$$V_{TAS_{stall}} = \sqrt{\frac{2mg_0}{C_{Lmax}\rho S}} \quad (3.6)$$

From this equation, to get the landing stall speed, the air density of sea level and landing configuration  $C_{Lmax}$  is used. For the same reason as in equation 3.4, the bank angle is assumed to be zero for the entire descent.

### 3.3.2 Clean configuration part

As stated before, for the clean configuration part, speed and the thrust are the controlled inputs. With this, the rate of descent has to be computed. From equation 3.1 we can obtain the rate of descent by isolating it as shown in equation 3.7. The drag is obtained from equation 3.3 and thrust is computed by BADA.

$$\frac{dh}{dt} = \frac{(T_{idle} - D)V_{TAS}}{mg_0} \left[ 1 + \left( \frac{V_{TAS}}{g_0} \right) \left( \frac{dV_{TAS}}{dh} \right) \right]^{-1} \quad (3.7)$$

In order to calculate the time of flight of the CDO the height will be integrated over time. The starting height is the height of the sequencing leg, which is the top of the descent phase. The final height is reached when a configuration change is required. However, as the speed change is not constant, because when the aircraft is descending with a constant CAS schedule the TAS speed varies over time due to the variation of air density. The integration has to be performed by numerical integration in order to overcome this issue. This means, starting with a defined initial speed and height at  $t_i$ ,  $\frac{dh}{dt}$  and  $\frac{dV_{TAS}}{dh}$  are obtained. These are added to the initial height and speed to get the input for  $t_{i+1}$ . This goes on until a configuration change is needed.

### 3.3.3 Non-clean configuration part

After the clean configuration part, the non-clean configuration part continues. This part starts when the configuration needs to be changed and goes until sea level. A configuration is needed when a certain speed and altitude limit is reached.

When the configuration change happens, the aircraft has to follow a flight path angle of three degrees to be able to intercept the glideslope of the ILS. As a result, to maintain the required flight path, thrust has to be increased to keep the speed defined in the speed schedule. The required thrust is obtained using equation 3.1. To introduce the flight path angle in this equation, equation 3.8 is used and equation 3.9 is obtained.

$$\frac{dh}{dt} = V_{TAS} \sin \gamma \quad (3.8)$$

$$(Thr - D) \cdot V_{TAS} = mg_0 V_{TAS} \sin \gamma + m V_{TAS} \frac{dV_{TAS}}{dt} \quad (3.9)$$

By rearranging some terms and assuming flight level at constant speed is maintained equation 3.10 is obtained.

$$Thr = D + mg_0 \sin \gamma + \frac{mg_0}{2\rho g_0} \frac{\partial \rho}{\partial h} V_{TAS}^2 \sin \gamma \quad (3.10)$$

The fuel flow can be obtained from BADA based on the computed thrust. The number of iterations defines the flight time and fuel consumption required to reach sea level from the sequencing leg. The fuel consumption is computed by the sum of the fuel flow at each iteration.

## CHAPTER 4. POINT MERGE SYSTEM DESIGN

In this chapter all the aspects studied before will be taken into account in order to achieve the project objective, the design of a Point Merge System at the Berlin-Schönefeld airport. The design will take place in the TMA of Berlin.

A TMA or Terminal Manoeuvring Area is the controlled airspace surrounding a major airport where there is a high volume of traffic. TMA airspace is normally designed in a circular configuration centered on the geographic coordinates of the airport, and differs from a control area in that it includes several levels of increasingly larger areas, creating an “upside-down wedding cake” shape [6].

Berlin-Schönefeld Airport, which can be seen in figure 4.1, is situated at the South-East of the city of Berlin and it is the secondary international airport of Berlin. In 2017 the airport handled 12.9 million passengers. Regarding its runways, the airport has only one runway, the 07L/25R.

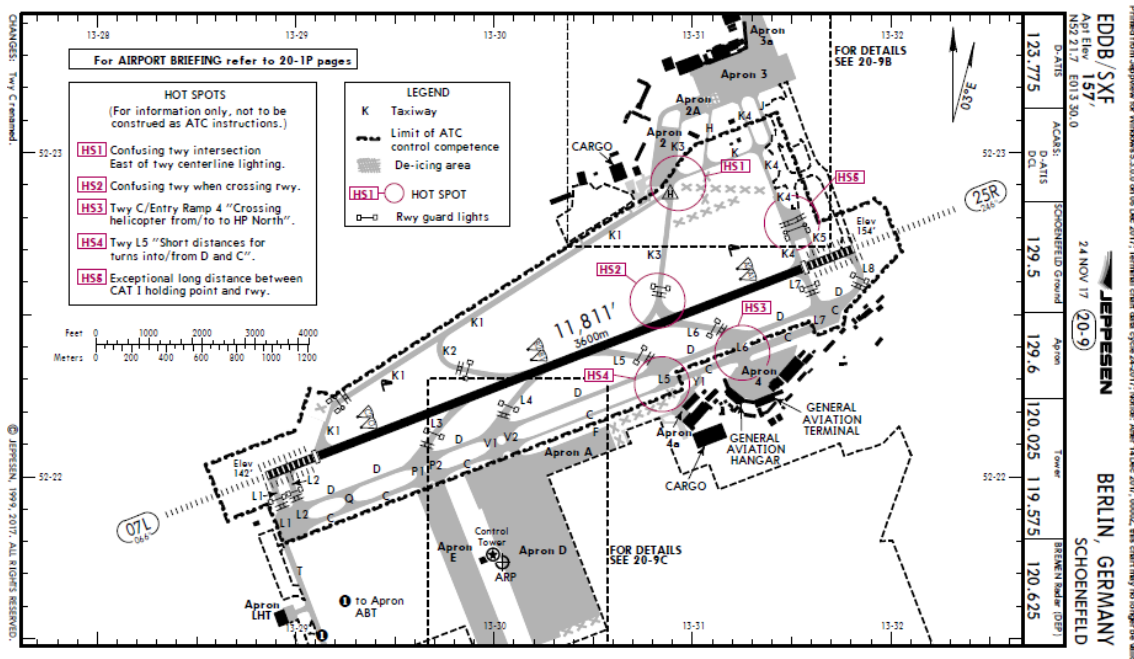


Figure 4.1: Berlin-Schönefeld airport

### 4.1 Requirements and Design Space

The design space is the available airspace for the implementation of the PMS. It has to be taken in mind that not the entire airspace is available. The airspace can be limited by restricted military airspace and the size of the TMA. In this project only runway 07L will be tested. The PMS will be designed for this runway.

To approach to the runway 07L aircraft enter the TMA at one of the two IAFs: LANUM or KLF at an altitude of 10,000ft. The IAFs are the starting points of the PMS design. The final point of the PMS design is the beginning of runway 07L. All airspace in between can be used for the design. Besides the design space, the following requirements of the design are identified by EUROCONTROL.

These requirements will be used for the design of the PMS at Berlin-Schönefeld.

- The design shall begin at the two IAFs and shall start at an altitude of 10,000ft.
- The full approach in the PMS shall fit in the current TMA, not interfering with the restricted airspaces and making implementation possible without major airspace changes.
- A three-degrees glide slope has to be obtained at least 10NM before the runway threshold in order to intercept the Instrument Landing System (ILS).
- The sequencing legs will be level and at least 20NM long, such as to have sufficient capacity to absorb delay.
- The leg between the sequencing leg and the Final Approach Fix (FAF) shall not have level segments, given the fact that the goal of the PMS is to implement CDOs which requires no level sections.
- To the extent possible, the route design should exhibit an overall symmetry in order to keep the operating method simple and intuitive.
- When multiple point merge systems are combined there must be a lateral offset between merge points to avoid the risk of head-on collisions.
- To the extent possible, the sequencing legs shall be approximately equidistant from the merge point, so that the sequencing legs are the same distance of the merge point.
- The sequencing leg shall be iso-distance from the merge point, so that at each point on the sequencing leg the distance to the merge point is equal.
- Parallel sequencing legs shall have a vertical separation of at least 1,000ft such as to have procedural separation.
- The parallel sequencing legs shall have at least a 1NM lateral separation to avoid ATC display cluttering.
- The design shall be in accordance with the terminal airspace design guidelines.
- The route structure shall not directly fly over heavily populated areas

## 4.2 Routes

In order to design the PMS the arrival and departure routes have been taken into account in order to make the design realistic and adapting it to the already existing routes making it a possible complement to the current procedures.

### 4.2.1 Arrival Routes

The arrival aircraft traffic in Berlin-Schönefeld for the runway 07L is divided in the arrivals from South and the arrivals from North (the current existing STARs can be seen in figure 4.2 and 4.3). Each arrival has an entry point called the IAF. Arriving aircraft merge to one of the two IAFs, which are named Klasdorf, for the traffic arriving from South, and Lanum for the traffic arriving from North. To transfer the aircraft from Air Traffic Services routes to one of the two IAFs, a Standard Terminal Arrival Route (STAR) is used, which is completely situated inside the CTA. The IAFs are the entry points of the aircraft into the TMA and the start of the approach segment of the aircraft.

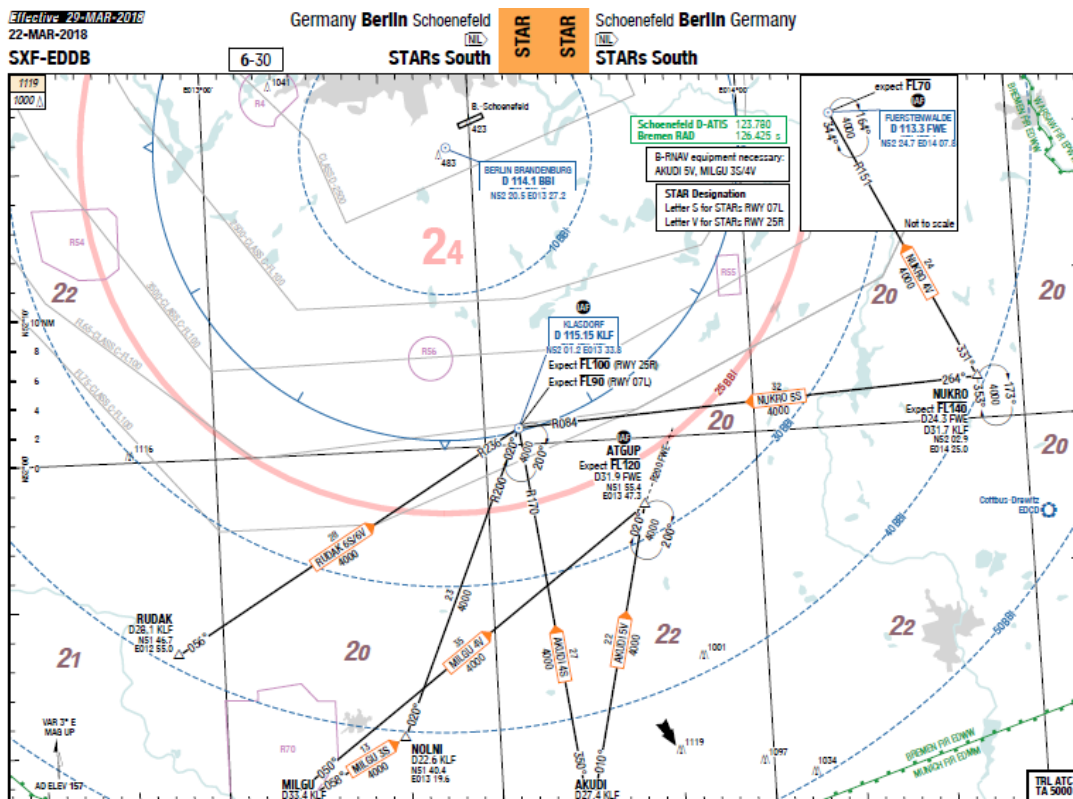


Figure 4.2: South STARs for Berlin-Schönefeld

### 4.2.2 Final Approach

In this project we will focus on the runway 07L and design the PMS for this runway taking into account the previous shown already existing routes. In order to make the design the last segment of the current final approach (figure 4.7) will be used.

The figure 4.4 corresponds to the actual ILS CAT II & CAT III or LOC for the runway 07L. There are two significant points, the Intermediate Fix (IF) named

DB552 and the Final Approach Fix named PIKOV situated at 8.8 nautical miles from the runway. At DB552 starts the intermediate approach leg which will end at the final approach fix. This leg's objective is to give the crew low workload in order to prepare the aircraft for landing. This leg is performed at 3000ft and it is straight. Then starting at PIKOV to the runway the final approach leg starts and the aircraft initiate the descending in a straight trajectory with a descend rate of  $3^{\circ}$ .

These two segments of the final approach (from DB552 to PIKOV to the runway) will be used in our design.

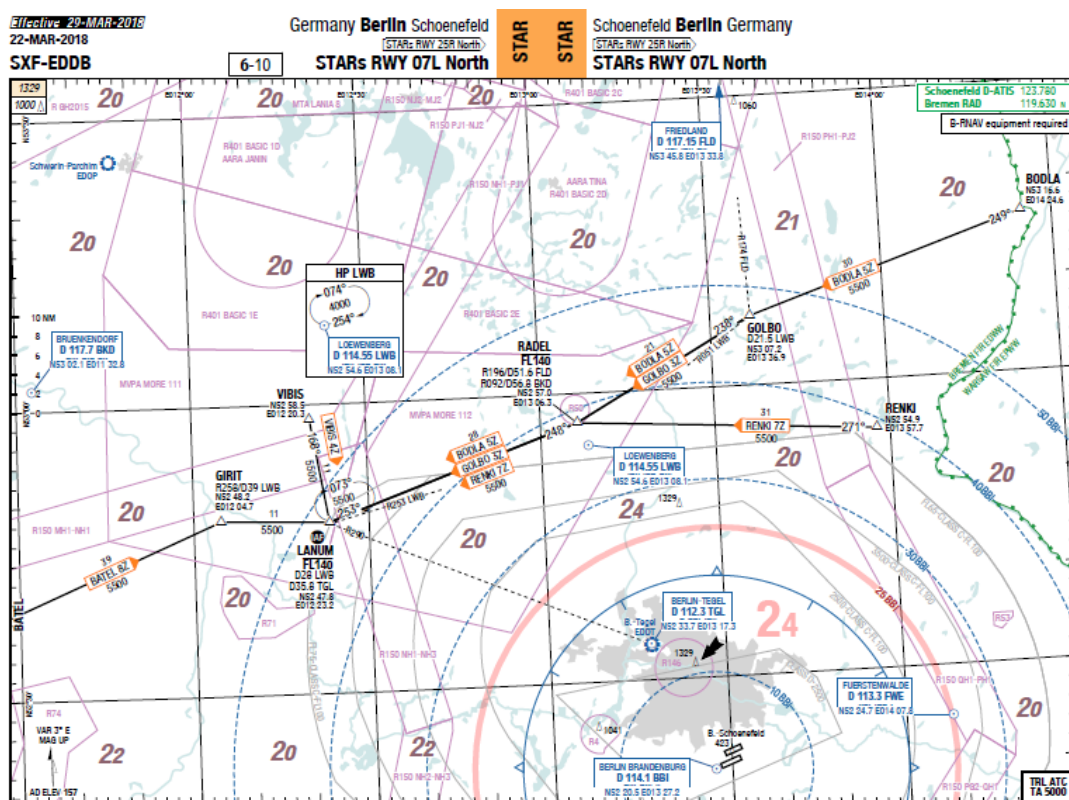


Figure 4.3: North STARs for Berlin-Schönefeld RWY 07L

### 4.3 Initial approach

The initial approach is the leg which will differ from the current existing approach. And it is where the Point Merge System will be applied taking into account all the parameters studied before.

Given the fact that all the incoming traffic for the runway 07L merges at two points, LANUM for the North arrivals and KLF for the South ones, a single point merge system composed by two arcs has been chosen. One arc will be used by the North traffic and the other for South.

Our PMS will be defined by the following dimensions:

- The arcs will be at 20NM of the merge point.
- The arcs will be separated 2NM between them.

- The arcs will be composed by 4 segments of 5NM each one.
- The merge point will be the existing DB552 point from which the aircraft will continue with the existing procedure.

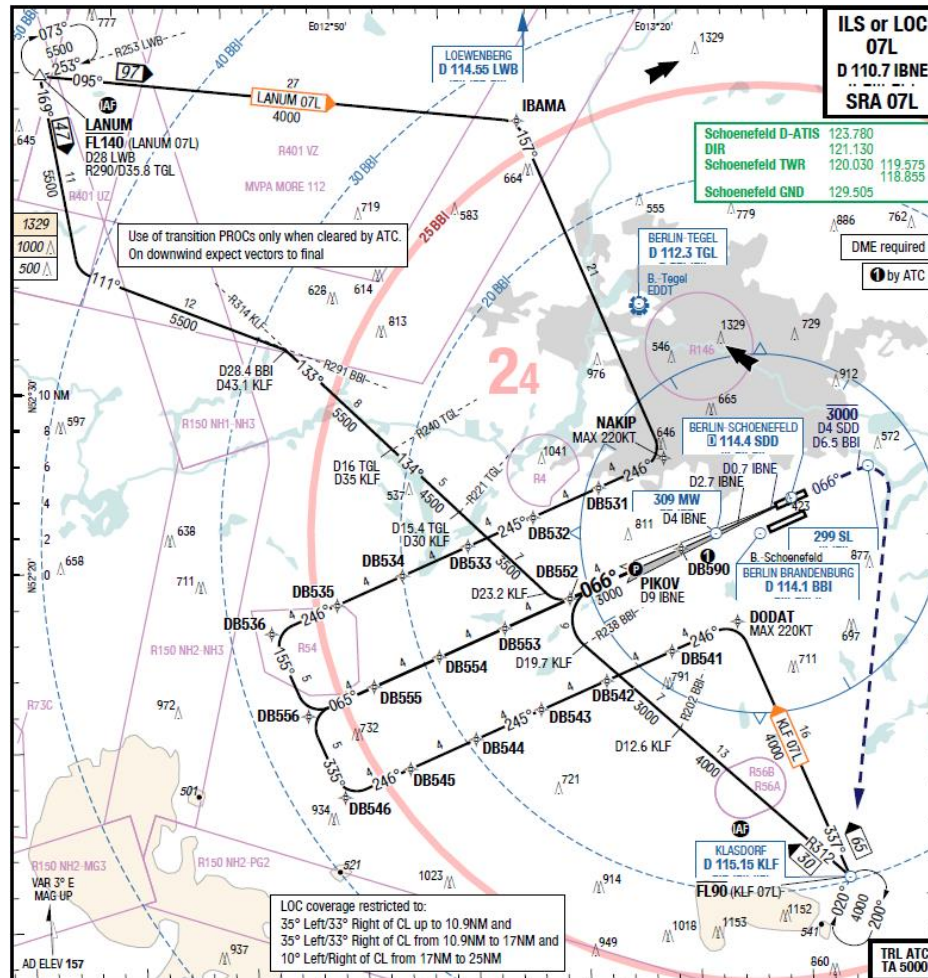


Figure 4.4: Final approach for Berlin-Schönefeld

#### 4.4 PMS Conceptual Design

The design of the PMS arcs will be defined.

The two arcs of our PMS will be placed at 20NM and 22NM from a merge point; in this case the merge point will be the existing point DB552. The PMS will have two entry points, one for each arc corresponding for either the North traffic or the South traffic.

Existing waypoint PIKOV is used as FAP, at an altitude of 3000ft, and waypoint DB552 as initial fix. The distance between DB552 and PIKOV is 4NM. The PMS requires two sequencing legs to be designed. It has been decided that the highest sequencing leg is set at an altitude of 10,000ft to keep the sequencing leg as high as possible. As a result of the requirements set, the second sequencing leg is positioned at an altitude of 9,000ft.

Given the fact that the altitude of the FAP is 3000ft, the altitude of the merge point shall not be very different since there is 4NM between the two points. It is known that this leg is probably the most complex scenario of the whole approach, since aside from correctly intercepting the ILS, the crew has to rightfully prepare the aircraft in altitude and speed. In this leg the required adjustments have to be minimized. Apart from that, a 1NM is required in order to guarantee a correct transition from RNP to conventional. Taking into account all the same altitude of 3000ft has been decided to be established at the Merge Point in order to give the crew the least workload possible.

A CDO is performed from the sequencing leg to the FAF, requiring a vertical descent of 7,000ft from the highest sequencing leg. As already mentioned, a sequencing leg with radius 20NM (the outer sequencing leg) has been chosen so the total distance from the sequencing leg to the FAF is 24NM. Descending 7,000ft within 24NM requires a descent rate of 291,7ft/NM, which is similar to the descent rate of other procedures. For the second leg a radius of 22NM has been chosen due to the fact that the inner sequencing leg should be at a higher altitude than the outer leg and to avoid ATC display cluttering the sequencing legs should have at least a lateral separation of 1NM. This helps reducing the risk of separation infringement in case an aircraft descends immediately after direct to instruction is given.

Regarding the speed at which the traffic will be limited at the PMS, the easiest scenario would be that all aircraft fly at a similar speed so that the separation management is simple. As previously discussed, the first phase for the air traffic controller is to create a lateral separation by extending the procedure, and the second phase is to manage this separation. For the first phase, the case in which all traffic is flying at the same speed is the optimum since it makes all the most intuitive possible for the controller. 220kt is a good speed to start the approach. We set the speed limitation at the entry points of the PMS at 220kts.

Once the incoming traffic reaches the Point Merge a new speed limitation is needed. If we take in mind that once the aircraft are placed in the final landing trajectory they are instructed to keep a speed of about 160kt until 4NM before the runway, a similar speed but a little bit higher will be the adequate. Before intercepting the localizer of the ILS there is a leg of about 4NM between the Merge Point and the FAP, with the sufficient margin to deaccelerate and descent to the altitude of 3000ft. A speed of 180kt is established at the FAP that will be decreasing as the aircraft gets closer to the runway. With this speed we also make sure that the controller has the necessary margin for the second phase of his procedure, to maintain the separation. Between the entry speed of 220kt and the exit speed of 180kt there is margin to make any needed adjustments in velocity.

One last issue regarding the altitudes and velocities is referring at how they must be performed by the crew. In his design document, EUROCONTROL requires that these limitations are of maximum speed and "at or below" altitude. We would like to narrow the possibilities of different velocities and altitudes at these points in order to reach the optimum performance and that the predictability of the systems remains unaffected. Therefore, all incoming traffic



## CHAPTER 5. MIXED INTEGER LINEAR PROGRAMMING FORMULATION

In this section a Mixed Integer Linear Programming model is proposed [4] to solve the aircraft scheduling problem in the Point Merge system.

In order to explain MILP formulation used in the scheduling model first a brief MILP overview is given. Second, the different sets and parameters that have been used for the MILP formulation are discussed. Third, the decision variables are presented. Fourth, the objectives functions are elaborated and finally the MILP constraints used in this research are explained.

### 5.1 Mixed Integer Linear Programming

The scheduling model for the PMS uses mixed integer linear programming in order to solve the problem. Integer Linear Programming is a mathematical optimization or feasibility program in which the objective function and the constraints are linear. The standard form for Integer Linear Programming is:

$$\begin{aligned} & \text{minimize } c^T x \\ & \text{subject to } Ax \leq b, \\ & x \geq 0 \end{aligned}$$

The aim of the program is to maximize, or minimize in this case, a linear function which is called the objective function. This function has the form of  $c^T x$ . The parameter  $c$  denotes the cost, which is coupled to a decision variable  $x$ . The parameter  $x$  is called the decision variable given the fact that it determines the cost increase or decrease. The decision variable is tied by a set of restrictions, called constraints. Two types of constraints exist. First, the functional constraints that are in the form of  $Ax \leq b$ . The functional constraints can be both equality and inequality constraints. Second, the non-negativity constraints, which assure the decision variable to be equal or greater than zero. The decision variable can be integer, binary or real-valued.

For the aircraft scheduling problem, the MILP formulation is widely used to solve the static case. The main advantage of MILP is that it is an exact method, which yields an optimal solution. The drawback of MILP is that for a large set of aircraft and constraints the computational time grows exponentially. To overcome the growth in computational time, exact solutions, heuristics, meta-heuristics and different solving techniques can be used. It has to be noted that the solution obtained using heuristics, meta-heuristics and other solution-techniques are feasible, but not necessarily the optimal solution. The solutions can result in a near optimal solution in a shorter computational time. In this project a practical algorithm of Constraint Position Shift (CPS) is implemented and the rolling horizon technique is applied to help reduce the computational time.

#### 5.1.1 Constraint Position Shift

The most common approach to sequencing aircraft [9] has been to maintain the First-Come-First-Served (FCFS) order. IN an FCFS schedule, aircraft land in

order of their scheduled arrival times at the runway, and air traffic controllers only enforce the minimum separation requirements. There are two key advantages to the FCFS sequence and landing time: first, the FCFS schedule is relatively easy to implement and promotes safety by reducing controller workload, and second, the FCFS order maintains a sense of fairness, since aircraft simply land in the order in which they arrive at the runway; the FCFS order also minimizes the standard deviation of delays of the aircraft.

However, a drawback of the FCFS sequence of landings is that it may lead to reduced runway throughput due to large spacing requirements. For example, a sequence of 10 alternating large and small aircraft will require greater spacing (and will therefore take more time to land overall) than one where 5 small aircraft are followed by 5 large aircraft. Air traffic controllers would like to complete landing a sequence of aircraft as quickly as possible, since the continued presence of aircraft in the sky contributes to a congestion and controller workload, and increase the associated risks. Low runway throughput leads to congestion around an airport and subsequent delays, compromising both safety and efficiency. This provides an incentive to deviate from the FCFS sequence to achieve sequences that lead to a maximum runway throughput. This is the basic motivation for Constrained Position Shifting (CPS) methods.

CPS, stipulates that an aircraft may be moved up to a specified maximum number of positions from its FCFS order. We denote the maximum number of position shifts allowed (also referred to as MPS) by  $k$ , and the resulting environment as a  $k$ -CPS scenario. An additional advantage of using CPS is that it maintains some sense of equity among the aircraft by not deviating too much from the FCFS order. Normally, the maximum number of position shifts in the sequence is three. In essence, the FCFS is a MPS of zero.

The closer the aircraft is to the runway, the less time there is available for switching positions and the more difficult it becomes. The technique of Relative Position Shift (RPS) defines a MPS depending on the position or place the aircraft has in the sequence. For example, closer to the runway the maximum position shift is lower than further away in the sequence.

This project uses the practical algorithms: FCFS and MPS. Limiting the aircraft to FCFS is used as a baseline to compare the PMS results to the current situation, where FCFS is used. A MPS of one and two position shifts will be used to examine the benefits obtained by allowing the sequence to be changed.

### **5.1.2 Rolling Horizon**

When there are a great number of flights, the landing time of the last aircraft does not influence the landing time of the aircraft as the landing times are far apart. If the timeline is long the interaction between these aircraft becomes negligible. Rolling horizon [8] focuses on reducing the computational time by introducing a time-horizon or event-horizon instead of solving the model for the entire aircraft set at once. An event-horizon is introduced to break down the entire timeline into several smaller sub-problems.

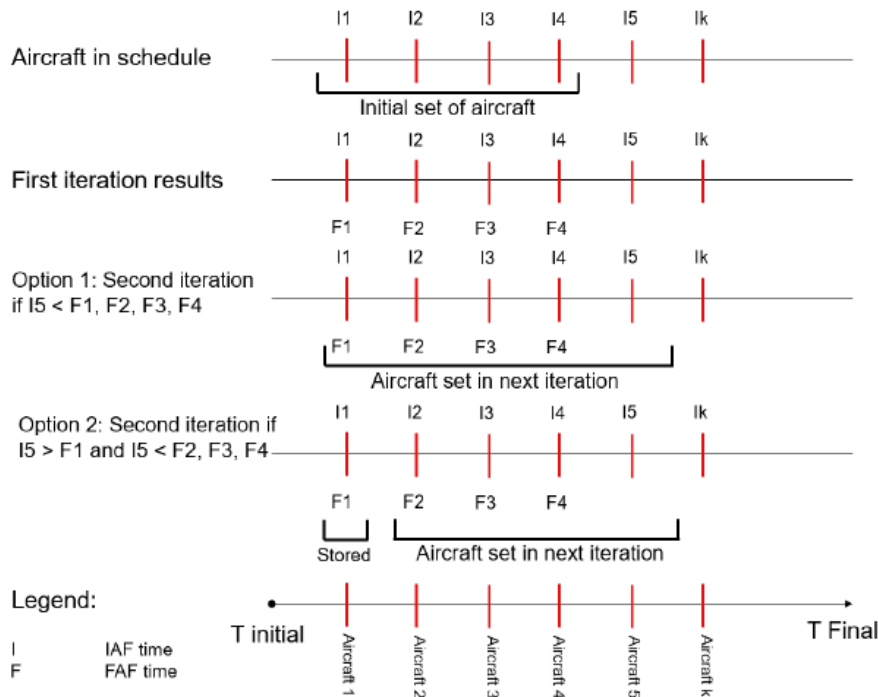


**Figure 5.1: Rolling Horizon example for FCFS [8]**

In figure 5.1 an illustrated example of the event based rolling horizon can be seen. A total set of  $k$  aircraft has to be scheduled (shown by the red lines). The IAF time of each aircraft is known and the total set is sorted by in the order of arrival at the IAF. First, a limited set of aircraft, denoted as the initial set of aircraft, is solved and a solution is found. The amount of initial aircraft is a manual input. A minimum of one aircraft can be used as initial set, up to a maximum of all aircraft in the set. For example, in figure 5.1, a set of 4 aircraft is chosen as initial set, shown in the first row. For the initial set, the schedule is optimized and the FAF times are obtained for each aircraft in the set. The following aircraft, in the total set of  $k$  aircraft, is added for the next iteration. In the example aircraft 5 is added. But based on the IAF time of aircraft 5 two options can occur:

1. The IAF time of aircraft 5 is earlier than the FAF times of the aircraft in the initial set. This means that when aircraft 5 enters the system, all preceding aircraft are still in the PMS. As a result, aircraft 5 is added to the initial set. The new set of 5 aircraft is used as set for the next iteration
2. The IAF time of aircraft 5 is later than the one or more FAF times of the aircraft in the initial set. The data of the aircraft with a FAF earlier than the IAF of the added aircraft are stored and the aircraft is removed from the next iteration. In the example, aircraft 5 has an IAF time later than the FAF time of aircraft 1. Therefore, aircraft 1 is removed from the next iteration and the output of the scheduling model of that aircraft is stored in a database.

After each iteration, the following aircraft in the total set of  $k$  aircraft is added, until the last aircraft, aircraft  $k$ , is added. The IAF time of the added aircraft is compared to the FAF times of the aircraft set performed in the prior iteration. When this IAF time is earlier than the FAF times of the aircraft in the set, a new iteration is performed (option 1). On the other hand, when the IAF time is alter than one or more FAF time of the aircraft in the set, the aircraft are removed and stored for the next set of aircraft (option 2). The window of aircraft slides because of the aircraft which are stored and not included into the next iteration, while a new aircraft is added each iteration. The rolling horizon method of figure 5.1 holds for the FCFS case. However, when position shift in the sequence is allowed, the case shown in figure 5.2 can occur.

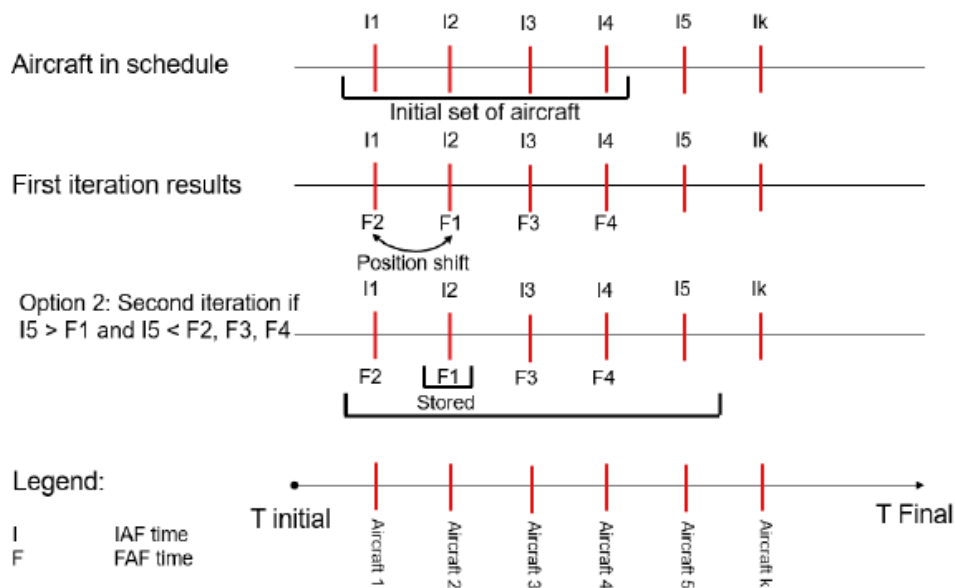


Figure 5.2: Rolling Horizon example for MPS [8]

In this case, a position shift takes place, switching the FAF times of aircraft 1 and 2. Aircraft 5 is added to the initial set, but now the IAF time of aircraft 5 is later than the FAF time of aircraft 2. However, aircraft 2 is not removed from the next iteration, because the trajectory of aircraft 1 depends on the trajectory of aircraft 2. Both aircraft 1 and 2 are removed only after the FAFs are both before the IAF time of new aircraft added to the set of aircraft.

## 5.2 Sets and parameters

The sets and parameters used in the MILP formulation will be shown. The MILP formulation uses the following sets:

$f \in F \equiv \{f_1, f_2, \dots, f_{N_f}\} = \text{set of all flights, where } N_f \text{ is the total number of flights.}$

$r \in R \equiv \{r_1, r_2, \dots, r_{N_r}\} = \text{set of all routes, where } N_r \text{ is the total number of routes.}$

$p \in P \equiv \{p_1, p_2, \dots, p_{N_p}\} = \text{set of all points, where } N_p \text{ is the total number of points.}$

Next, the parameters comprised by the MILP formulation of the scheduling problem:

$P_F$ : final point (FAF).

$P_I$ : initial point of the PMS (entry point of the sequencing leg).

$P_T$ : Actual point on the sequencing leg where the aircraft turns towards the merge point.

$T_f^{IAF}$ : IAF arrival time in seconds of aircraft  $f$ .

$T_{f,r}^{CDA}$ : Total duration in seconds of the CDA procedure for aircraft  $f$  on route  $r$ .

$V_{f,r,p}^{max}$ : Maximum true airspeed in knots allowed for aircraft  $f$  on route  $r$  at point  $p$ .

$V_{f,r,p}^{min}$ : Minimum true airspeed in knots allowed for aircraft  $f$  on route  $r$  at point  $p$ .

$d^{leg}$ : Discrete distance in nautical miles between turn points on the sequencing leg.

$d_{r,P_I}^{initial}$ : Distance in nautical miles from the IAF to the initial point of the PMS on route  $r$ .

$d_{f,r}^{turn}$ : Total distance from the entry point to the turn point for aircraft  $f$  on route  $r$ .

$d_r^{seq}$ : Maximum length of the sequencing leg for route  $r$  in miles.

$SEP_{f,f'}$ : Minimum wake vortex separation in NM between leading aircraft and trailing aircraft  $f'$ .

$V_{initial_f}$ : Initial true airspeed of aircraft  $f$  in the initial segment of the PMS.

$V_{leg_f}$ : The sequencing leg true airspeed of aircraft  $f$ .

$V_{final_f}$ : The final approach true airspeed of aircraft  $f$ .

### 5.3 Decision variables

Once the sets and parameters have been identified the following decision variables are defined:

$A_{f,r}$  = A binary value which is 1 if aircraft  $f$  is assigned to route  $r$  and zero otherwise.

$T_{f,r,p}$  = A real variable which represents at which time, flight  $f$  on route  $r$  arrives at point  $p$ .

$S_{f,f',r,r',p}$  = A binary variable which is 1 when flight  $f$  on route  $r$  is before flight  $f'$  on route  $r'$  at checked point  $p$ .

$Z_{f,r,p}$  = A real variable which represents the fuel used by flight  $f$  on route  $r$  at point  $p$ .

## 5.4 Objective function

In this section two objective functions will be defined. The first objective function aims at minimizing the makespan. This is the total time span between the landing time of the first aircraft in the sequence and the landing time of the last aircraft in the sequence. By minimizing the makespan the runway throughput is maximized. The second objective function aims at minimizing the sum of the total fuel each aircraft consumes. This relates to the environmental impact as more fuel used causes more emissions.

### 5.4.1 Minimize makespan

The performance index of this optimization problem is shown in equation 5.1. The total sum of final time is minimized. For all aircraft in the set and all routes in the set, the time at the final point  $p_F$  is summed, but only if the aircraft flies over that particular route  $A_{f,r}$ .

$$J = \min \sum_{f \in F} \sum_{r \in R} A_{f,r} T_{f,r,p_F} \quad (5.1)$$

This equation is not linear as it is a product of two variables. The variable  $A_{f,r}$  is a logical value which is binary while  $T_{f,r,p_F}$  is a real-continuous value. By introducing an auxiliary variable, the objective function can be converted into a linear function. The following variable is introduced:

$$\delta_{f,r,p_F}^T \triangleq A_{f,r} T_{f,r,p_F} \quad (5.2)$$

Along with the following set of equations, the objective function is converted into a linear function using the so-called big M approach:

$$\delta_{f,r,p_F}^T \geq T_{f,r,p_F} - M(1 - A_{f,r}) \quad (5.3)$$

$$\delta_{f,r,p_F}^T \leq T_{f,r,p_F} + M(1 - A_{f,r}) \quad (5.4)$$

where  $M$  is an arbitrarily large number.

### 5.4.2 Minimize total fuel consumed

The objective function is shown in equation 5.5.  $Z_{f,r,p_F}$  denotes the total fuel consumed at the final point. In this project the fuel consumed can vary due to the fact that variable speed and variable time in the sequencing leg can occur. The total fuel consumed comprises the fuel consumed in the initial, sequencing and CDA segment.

$$J = \min \sum_{f \in F} \sum_{r \in R} Z_{f,r,p_F} \quad (5.5)$$

Both equation 5.5 and equation 5.2 can be combined to optimize both fuel burned and makespan. A weight factor  $w \in [0,1]$  is added to combine the two equations and to see the effect when making one criterion more important than the other. The combined objective function is shown in equation 5.6:

$$J = \min \sum_{f \in F} \sum_{r \in R} w^z \cdot Z_{f,r,p_F} + w^T \cdot \delta_{f,r,p_F}^T \quad (5.6)$$

where  $w^z = w$

$$w^T = (1 - w)$$

## 5.5 Constraints

In this section, the constraints of the scheduling model in MILP formulation are explained; eight sets of constraints are included into the model.

### 5.5.1 Single Route

The first constraint assures that at least one route is assigned to each aircraft and that only one route is assigned to each aircraft.

$$\sum_{r \in R} A_{f,r} = 1 \forall f \in F \quad (5.7)$$

### 5.5.2 Initial Leg Time and Speed

Before the aircraft enters the PMS, the initial segment is flown from the IAF to the entry point of the PMS. The airspeed on this segment can vary, which affects the entry time of the aircraft in the system. This constraint is shown in equation 5.8.

$$A_{f,r}(T_{f,r,p_1} - T_{f,r,p_1}^E) \geq 0, \forall f \in F, \wedge \forall r \in R^f \quad (5.8)$$

If a flight is assigned to route A, the initial time at the first point in the PMS is greater or equal to a specified minimum initial time. This equation is also non-linear, but by introducing an auxiliary variable  $\delta_{f,r,p_1}^T$ , as in equation 5.3 and 5.4, equation 5.8 is converted to a linear form shown in equation 5.9.

$$\delta_{f,r,p_1}^T - A_{f,r}T_{f,r,p_1}^E \geq 0, \forall f \in F, \wedge \forall r \in R^f \quad (5.9)$$

The parameter  $T_{f,r,p_1}^E$  is the earliest time the aircraft can arrive at the entry point and is calculated using equation 5.10. The earliest time the aircraft can be in the PMS is when it flies its maximum allowed speed, which is calculated as in section 3. Thus  $T_{f,r,p_1}^E$  is the IAF time of the aircraft, plus the distance in nautical miles to the initial point of the PMS divided by the maximum true airspeed in knots.

$$T_{f,r,p_1}^E = T_f^{IAF} + \frac{d_{r,p_1}^{initial} \cdot 60 \cdot 60}{V_{f,r,p}^{max}} \quad (5.10)$$

This is the earliest time the aircraft can be in the PMS, but there is also a minimum speed the aircraft can fly. Therefore, a constraint is added for the latest time an aircraft can arrive at the entry point ( $T_{f,r,p_1}^L$ ). This can be seen in equation 5.11.

$$\delta_{f,r,p_1}^T - A_{f,r}T_{f,r,p_1}^L \leq 0, \forall f \in F, \wedge \forall r \in R^f \quad (5.11)$$

Instead of the maximum speed now the minimum speed is used to compute the latest time the aircraft can be at the PMS. This can be seen in equation 5.12.

$$T_{f,r,p_l}^L = T_f^{IAF} + \frac{d_{r,p_l}^{initial} \cdot 60 \cdot 60}{V_{f,r,p}^{min}} \quad (5.12)$$

The earliest and latest time differ per aircraft type, as the maximum speed and minimum speeds are different for each aircraft type. But it also changes per sequencing leg, as the height of the sequencing leg also influences the minimum and maximum speeds. AS the initial speed can variate between the minimum and maximum speed, the actual speed flown by the aircraft has to be determined to calculate the fuel consumed. Bases on the segment length from the IAF to the PMS the actual speed flown can be calculated as in equation 5.13.

$$\delta_{f,r,p_l}^T - A_{f,r} T_f^{IAF} - \frac{d_{r,p_l}^{initial} \cdot 60 \cdot 60}{V_{initial_f}} = 0, \forall f \in F, \wedge \forall r \in R^f \quad (5.13)$$

### 5.5.3 Sequencing Leg Time and Speed

The velocity of the aircraft in the sequencing leg can vary as well. This means that the aircraft can be earlier or later at the turn-point of the flown route. Given the fact that both distance to the turn-point and speed are variable, the sequencing leg is discretized into segments of 1 nautical mile in length, to have at least one parameter fixed. An example PMS discretized into three segments of 1NM can be seen in figure 5.3.

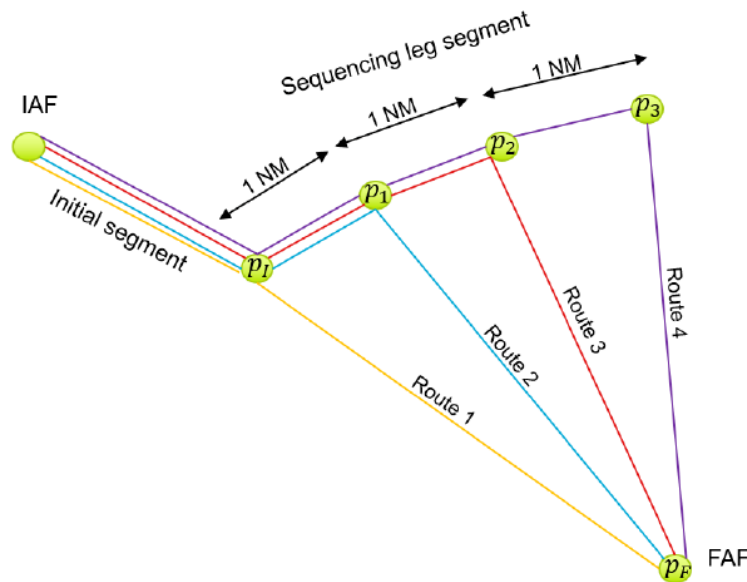


Figure 5.3: PMS discretised in segments of 1NM [4]

It can be seen that aircraft fly a common initial segment, but after the entry point ( $P_1$ ), the aircraft can be given the instruction to fly four different routes, depending on the required separation. For route 1, the turn-point is  $P_1$ , for route 2 the turn-point is  $P_1$ , etc. The velocity along the sequencing leg can vary, however, due to the fact that this speed is constant, the minimum and maximum

travel time to each turn-point for each route can be computed. The next equation represents the constraint for minimum time to travel from the entry point  $P_I$  to the turn-point  $p$  of route  $r$ .

$$A_{f,r}(T_{f,r,p_T} - T_{f,r,p}^E) \geq 0, \forall f \in F, \forall r \in R^f \quad (5.14)$$

And by using an auxiliary variable  $\delta_{f,r,p_T}^T$  for each turn-point on the sequencing leg, the equation 5.14 is transformed into a linear form. This establishes the travel time from  $P_I$  to the turn-point of each route. By substituting the auxiliary variable  $\delta_{f,r,p_T}^T$  in the previous equation, equation 5.15 is obtained.

$$\delta_{f,r,p_T}^T - A_{f,r}T_{f,r,p}^E \geq 0, \forall f \in F, \forall r \in R^f \wedge \forall p \in P^r \quad (5.15)$$

The earliest time the aircraft can be on the turning-point depends on the distance from the entry point to the corresponding turning-point and also depends on the maximum true airspeed of the aircraft type. This constraint is shown in equation 5.16.

$$T_{f,r,p}^E = \sum_{p_I}^{p_T} \frac{d_{leg} \cdot 60 \cdot 60}{V_{f,r,p}^{max}} \forall p \in P^r, p \leq p_L \quad (5.16)$$

The distance between the entry point and the turn-point is the sum of each segment before the turn-point, where the distance of each segment ( $d_{leg}$ ) is 1NM. In the example shown in figure 5.3, the distance on the sequencing leg of route 4 is the summation of the distance between  $P_I$  and  $P_1$ , plus the distance between  $P_1$  and  $P_2$ , plus the distance between  $P_2$  and  $P_3$ . It has to be taken in mind that the maximum true airspeed differs for each aircraft type and the altitude of the sequencing leg.

Exactly the same method used to compute the minimum travel time is used to calculate the maximum travel time. But instead of using the maximum speed, in this case, the minimum true airspeed is used. By replacing the earliest travel time for the latest travel time equations 5.17 and 5.18 are obtained.

$$\delta_{f,r,p_T}^T - A_{f,r}T_{f,r,p}^L \leq 0, \forall f \in F, \forall r \in R^f \wedge \forall p \in P^r \quad (5.17)$$

$$T_{f,r,p}^L = \sum_{p_I}^{p_T} \frac{d_{leg} \cdot 60 \cdot 60}{V_{f,r,p}^{min}} \forall p \in P^r, p \leq p_L \quad (5.18)$$

Ultimately, the actual true airspeed flown by the aircraft on the sequencing leg has to be computed for the fuel consumption. The true airspeed on the sequencing leg is equal to the travel time at the turn-point divided by the distance between the entry point and the turn-point. This can be seen in equation 5.19. The speed is obtained in knots.

$$\frac{\delta_{f,r,p_T}^T}{\sum_{p_I}^{p_T} d_{leg}} - \frac{60 \cdot 60}{V_{legf}} = 0, \forall f \in F, \forall r \in R^f, \forall p \in P^r \wedge p \leq p_L \quad (5.19)$$

### 5.5.4 Continuous Descent Approach time and speed

Once the sequencing leg segment has been flown, the CDO segment starts. Again, the time and speed have to be computed for this segment. There is only one CDO profile for each route the aircraft can fly, which is the ideal CDO profile. The CDO profile differs for each aircraft type and sequencing leg. The constraint for travel time in the CDO segment is shown in equation 5.20.

$$T_{f,r}^{CDA} = A_{f,r} T_{CDA_{f,r}} \forall f \in F, \wedge \forall r \in R^f \quad (5.20)$$

The CDO travel time from the turn-point to the FAF is denoted as  $T_{CDA_{f,r}}$  in equation 5.20.

### 5.5.5 Ordering Constraint

In order to compute the separation needed between aircraft, first, the order in which the aircraft are sequenced has to be determined. For each pair of flights travelling on the same route or a different route with shared common scheduling points, the order has to be determined. The general equation to determine this order at shared points is shown in equation 5.21.

$$S_{f,f',r,r',p} + S_{f',f,r',r,p} = A_{f,r} A_{f',r'} \quad (5.21)$$

$$\forall f, f' \in F, f \neq f', \forall r \in R^f, \forall r' \in R^{f'}, \forall p \in [P^r \cap P^{r'}] \neq \emptyset$$

The variable  $S_{f,f',r,r',p}$  is a binary number which is 1 when flight  $f$ , travelling on route  $r$  is in front of flight  $f'$ , travelling on route  $r'$ , analyzed at all shared points  $p$ . Equation 5.21 is non-linear, therefore, following the same method used previously, an auxiliary variable  $\delta_{f,f',r,r'}^A$  is introduced to obtain a linear form.

$$\delta_{f,f',r,r'}^A \triangleq A_{f,r} A_{f',r'} \quad (5.22)$$

By substituting this auxiliary variable into equation 5.21, equation 5.23 is obtained. This is a linear equation where  $\delta_{f,f',r,r'}^A$  is a product of two logical variables subjected to the set of constraints of equations 5.24, 5.25 and 5.26.

$$S_{f,f',r,r',p} + S_{f',f,r',r,p} = \delta_{f,f',r,r'}^A \quad (5.23)$$

$$-A_{f,r} + \delta_{f,f',r,r'}^A \leq 0 \quad (5.24)$$

$$-A_{f',r'} + \delta_{f,f',r,r'}^A \leq 0 \quad (5.25)$$

$$A_{f',r'} + A_{f,r} - \delta_{f,f',r,r'}^A \leq 1 \quad (5.26)$$

$$\forall f, f' \in F, f \neq f', \forall r \in R^f, \forall r' \in R^{f'}, \forall p \in [P^r \cap P^{r'}] \neq \emptyset$$

As the order can only be changed once in the PMS, only the order at the entry point ( $P_I$ ) and the final point ( $P_F$ ) has to be checked. The order is changed if the trailing aircraft turns towards the merge point earlier than the leading aircraft. The order at the entry point and final point can be calculated using equation 5.27 and 5.28 respectively.

$$S_{f,f',r,r',p_I} + S_{f',f,r,r',p_I} = \delta_{f,f',r,r'}^A \quad (5.27)$$

$$\forall f, f' \in F, f \neq f', \forall r \in R^f, \forall r' \in R^{f'} \wedge \forall r = r'$$

$$S_{f,f',r,r',p_F} + S_{f',f,r,r',p_F} = \delta_{f,f',r,r'}^A \quad (5.28)$$

$$\forall f, f' \in F, f \neq f', \forall r \in R^f, \forall r' \in R^{f'}$$

Due to the fact that the sequencing legs are at different altitude, the entry point order of the PMS is only relevant for aircraft in the same system and sequencing leg. However, all aircraft have a common final point, the FAF of the runway used for landing.

To incorporate the FCFS order constraint, an extra constraint is introduced at the final point to force  $S_{f,f',r,r',p_F}$  to 1 preventing aircraft from switching position in the sequence. Note that, the parameter  $S_{f,f',r,r',p_F}$  only denotes the sequence between a pair of aircraft, but does not imply that a given aircraft is positioned directly prior to or after its pair. It only shows that an aircraft is sequenced some time prior to or after its pair. For implementing MPS, the  $T_f^{IAF}$  of the trailing aircraft  $f'$  behind the leading aircraft  $f$  are sorted to know the immediate order behind the aircraft  $f$ . The aircraft  $f'$  within the allowed maximum position shift uses the normal ordering constraint as in equation 7.28. However, for the aircraft positioned outside the allowed maximum positions shift, the parameter  $S_{f,f',r,r',p_F}$  is forced to 1 meaning that the trailing aircraft  $f'$  cannot overtake aircraft  $f$  in the sequence. Note that the maximum number of allowed position shifts is a manual input.

### 5.5.6 Separation

Another important aspect is to maintain the separating between aircraft. The separation requirements are discussed in this section. In the PMS, the vertical and lateral separation requirements are maintained by design. Therefore, only longitudinal separation violations can occur in the PMS, such as trailing conflicts depicted in figure 5.4. Trailing conflicts occur when the trailing aircraft catches up the leading aircraft due to a speed difference.

It is assumed that aircraft are sufficiently separated when entering the TMA. They fly at a constant speed in each segment of the PMS, however the speed between aircraft in the same segment can be different. Therefore, the separation requirements have to be checked at each point a speed change occurs. The potential conflicting points can be identified next:

- At the entry point of the PMS ( $p_I$ ). As the initial segment is a common path and aircraft can fly at different airspeeds, trailing conflicts can occur.
- At the FAF point of the PMS ( $p_F$ ). AS in the CDO segment the aircraft merge to one point, there is a risk of trailing conflicts at the merge point
- Over the common path on the sequencing leg. As aircraft can have different speeds on the sequencing leg, there is a risk of a trailing

conflict. The common path is important, because depending on the route the aircraft take, the common path differs for each aircraft.

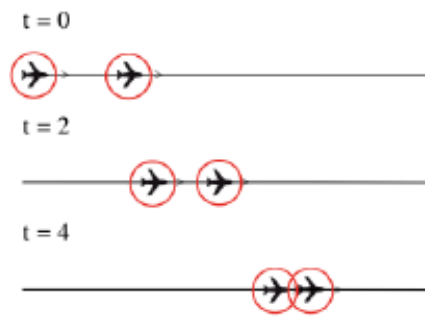


**Figure 5.4: Two potential loss of separation conflicts: (a) cross conflict, (b) trailing conflict [4]**

The minimum longitudinal separation distance required is based on the ICAO vortex separation distances [1]. This subsection, first explains the separation constraints at the entry point and FAF of the PMS. Then, the separation constraints on the sequencing leg are identified.

#### 5.5.6.1 Separation at the entry point and FAF

The longitudinal separation is checked at the entry point for both arriving and departing flights as depicted in figure 5.5. The aircraft are required to be at least the vortex longitudinal separation distance in miles separated measured at the entry point ( $P_I$ ). Due to the fact that aircraft fly at different speeds, the distance based separation standards are converted to a time based separation standards by dividing it by the airspeed. Two conditions have to be checked:

- First, if the aircraft  $f$  arrives at the entry point ( $P_I$ ), the trailing aircraft  $f'$  should arrive at least the minimum vortex separation time later at the entry point. The minimum vortex separation time depends on the minimum vortex separation distance between aircraft  $f$  and  $f'$  ( $SEP_{f,f'}$ ) and the initial segment airspeed of trailing aircraft  $f'$  ( $V_{initial_{f'}}$ ). This is called the separation between aircraft  $f$  and  $f'$  for arriving at point  $p$ .
- Second, if aircraft  $f'$  arrives at the entry point ( $P_I$ ), the leading aircraft should be at least the minimum separation time later from the entry point. However, now the minimum vortex separation time depends on  $SEP_{f,f'}$  and the sequencing leg segment airspeed of trailing aircraft  $f'$  ( $V_{leg_{f'}}$ ). This is called the separation between aircraft  $f$  and  $f'$  for departing point  $p$ .

In the MILP formulation, the first condition is ensured with equation 5.29 and the second condition is ensured by equation 5.30. It can be seen that the critical condition is the case where the largest minimum vortex separation time is required.

$$A_{f',r'}T_{f',r',p_I} \geq A_{f,r}T_{f,r,p_I} + \frac{SEP_{f,f'}}{V_{initial_{f'}}} - M(1 - S_{f,f',r,r',p_I}) \quad (5.29)$$

$$A_{f',r'}T_{f',r',p_I} \geq A_{f,r}T_{f,r,p_I} + \frac{SEP_{f,f'}}{V_{leg_f}} - M(1 - S_{f,f',r,r',p_I}) \quad (5.30)$$

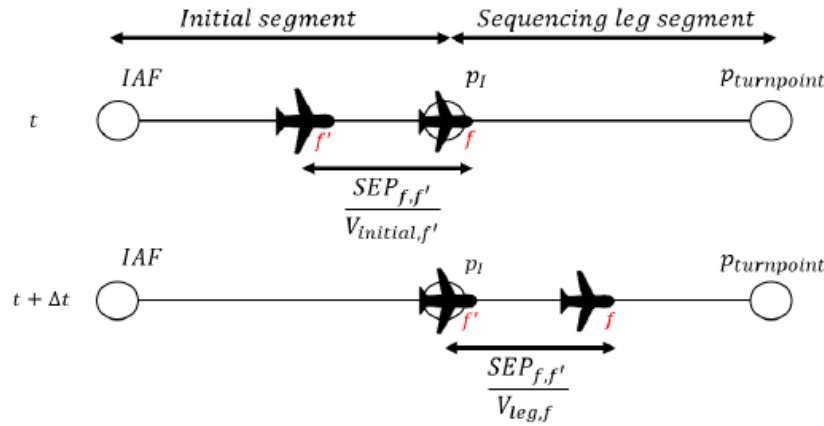


**Figure 5.5: Separation checked between aircraft f and f', arriving and departing a point p [4].**

The same method is used for the FAF separation to ensure the longitudinal vortex separation requirements, except now the final approach speed of aircraft is taken ( $V_{final_f}$ ). The set of constraints for this situation is expressed in equation 5.31 and 5.32.

$$A_{f',r'}T_{f',r',p_F} \geq A_{f,r}T_{f,r,p_F} + \frac{SEP_{f,f'}}{V_{final_{f'}}} - M(1 - S_{f,f',r,r',p_F}) \quad (5.31)$$

$$A_{f',r'}T_{f',r',p_F} \geq A_{f,r}T_{f,r,p_F} + \frac{SEP_{f,f'}}{V_{final_f}} - M(1 - S_{f,f',r,r',p_F}) \quad (5.32)$$

#### 5.5.6.2 Separation over the sequencing leg

Regarding the sequencing leg, the separation only needs to be checked at the common path of the aircraft pair on the same sequencing leg. The constraint for maintaining the minimum vortex separation time required over this sequencing leg follows the same principle as the entry point and FAF. This is due to the different possible turn-points the aircraft can use to increase the separation distance. Being said so, three situations (graphically described in figure 5.6) can occur when a pair of leading aircraft f and trailing aircraft f' are both flying over the same sequencing leg:

1. Aircraft f has a turn-point before the turn-point of aircraft f' on the sequencing leg.
2. Aircraft f' has a turn-point before the turn-point of aircraft f on the sequencing leg.
3. Aircraft f and aircraft f' turn at the same point on the sequencing leg.

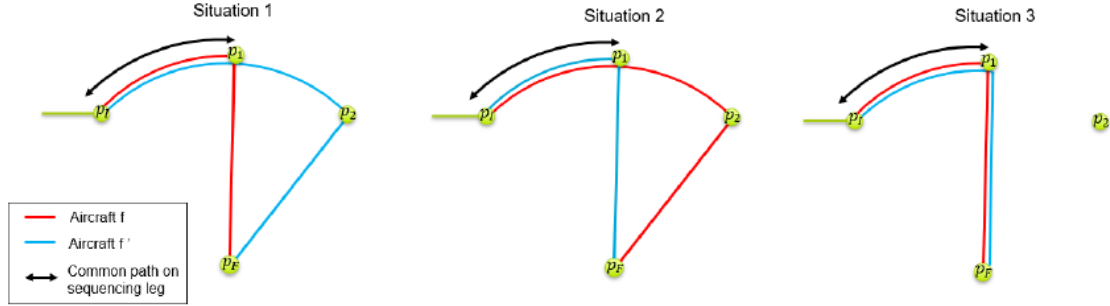


**Figure 5.6: Three situation which can occur between a pair of aircraft on the sequencing leg [4].**

For each one of these situations the separation has to be checked at the end of the common path, which is the turn-point of the aircraft turning first. Three slack variables are introduced to identify which one of the three situations is happening. For situation 1, binary slack variable  $S_{turn_{f,r}}$  is introduced. The variable is 1 when the turn-point of aircraft f is before the turn-point of aircraft f'. For situation 2, another binary slack variable is introduced;  $S_{turn_{f',r'}}$ , it is 1 when the turn point of aircraft f' is before the turn point of aircraft f. For situation 3, both  $S_{turn_{f,r}}$  and  $S_{turn_{f',r'}}$  are 0. An additional variable  $S_{equal_{f,r}}$  is added, which is 1 when the aircraft turn at the same turn-point on the sequencing leg. The following constrains are obtained:

- For situation 1:

$$\frac{d_{f,r}^{turn} A_{f,r}}{d_r^{seq}} - \frac{d_{f',r}^{turn} A_{f',r}}{d_r^{seq}} + S_{turn_{f,r}} \geq 0 \quad (5.33)$$

- For situation 2:

$$\frac{d_{f',r}^{turn} A_{f',r}}{d_r^{seq}} - \frac{d_{f,r}^{turn} A_{f,r}}{d_r^{seq}} + S_{turn_{f',r'}} \geq 0 \quad (5.34)$$

- For situation 3: This constraint is added to make sure that in this case the  $S_{equal_{f,r}}$  becomes 1 when  $S_{turn_{f,r}}$  and  $S_{turn_{f',r'}}$  are both 0.

$$S_{turn_{f,r}} + S_{turn_{f',r'}} + S_{equal_{f,r}} = 1 \quad (5.35)$$

Given the fact that the order on the sequencing leg is the order at which the aircraft arrive into the system, for each situation the initial order ( $S_{f,f',r,r',P_1}$ ) is multiplied with the variables introduced in equations 5.33, 5.34 and 5.35. As this is not a linear form, but a product of two logical variables, an equivalent set of equations is added.

$$S_{turn_{f,r}} \cdot S_{f,f',r,r',P_I} = \delta_{f,f',r,r',P_T}^S \quad (5.36)$$

$$S_{turn_{f',r'}} \cdot S_{f,f',r,r',P_I} = \delta_{f',f,r,r',P_T}^S \quad (5.37)$$

$$S_{equal_{f,r}} \cdot S_{f,f',r,r',P_I} = \delta_{f,f',r,r',P_T}^S \quad (5.38)$$

Situation 1 is true if  $\delta_{f,f',r,r',P_T}^S$  of equation 5.36 is 1, in this case the leading aircraft turns prior to the trailing aircraft on the sequencing leg. Situation 2 is true if  $\delta_{f',f,r,r',P_T}^S$  of equation 5.37 is 1. In this case the trailing aircraft turns at a point prior to the turn-point of the leading aircraft. Situation 3 is true if  $\delta_{f,f',r,r',P_T}^S$  of equation 5.38 is 1, when the turn-point of the leading and trailing aircraft are at the same point.

For each of the three situations, the point where the common path on the sequencing leg ends is where the separation requirements is checked.

For situation 1, the common path ends at the turn-point of aircraft f. There is one general assumption for all situations, once an aircraft turns, it is off the sequencing leg and no separation has to be checked after the aircraft turns. The separation constraint for situation 1 is shown in equation 5.39.

$$A_{f',r'} T_{f',r',P_I} + \frac{A_{f,r} d_{f,r}^{turn}}{V_{leg_{f'}}} \geq A_{f,r} T_{f,r,P_T} + \frac{SEP_{f,f'}}{V_{leg_{f'}}} - M \left( 1 - \delta_{f,f',r,r',P_T}^S \right) \quad (5.39)$$

The left-hand-side of this equation can be expressed as the time at which aircraft f' arrives at the turn-point of aircraft f. This is equal to the entry time of aircraft f' plus the distance on the sequencing leg to the turn point of aircraft f divided by the speed of aircraft f'. This side of the equation must be equal or bigger than the turn-time of aircraft f plus the minimum required vortex separation time between aircraft f and f'. Only the separation requirement for aircraft f' arriving at the turn-point of aircraft f has to be checked, due to the constraint that once an aircraft turns it is off the sequencing leg.

For situation 2, aircraft f continues over the sequencing leg after the aircraft f' turns. Therefore, in this situation both the separation requirement of aircraft departing and arriving at the turn-point of aircraft f' has to be checked. Equations 5.40 and 5.41 show the separation constraints for situation 2.

$$A_{f',r'} T_{f',r',P_T} \geq A_{f,r} T_{f,r,P_I} + \frac{A_{f',r'} d_{f',r}^{turn}}{V_{leg_f}} + \frac{SEP_{f,f'}}{V_{leg_{f'}}} - M \left( 1 - \delta_{f',f,r,r',P_T}^S \right) \quad (5.40)$$

$$A_{f',r'} T_{f',r',P_T} \geq A_{f,r} T_{f,r,P_I} + \frac{A_{f',r'} d_{f',r}^{turn}}{V_{leg_f}} + \frac{SEP_{f,f'}}{V_{leg_{f'}}} - M \left( 1 - \delta_{f',f,r,r',P_T}^S \right) \quad (5.41)$$

For situation 3, when both aircraft turn at the same point the separation requirement is checked using the same method as for the entry point and the FAF and is shown in equation 5.42. The turn-time of aircraft f' must be larger than the turn-time of aircraft f plus the required vortex separation time.

$$A_{f',r'}T_{f',r',P_T} \geq A_{f,r}T_{f,r,P_T} + \frac{SEP_{f,f'}}{V_{leg_{f'}}} - M(1 - \delta_{f,f',r,r',P_T}^S) \quad (5.42)$$

### 5.5.7 Total Transit Time

One of the decision variables included into the objective function is the total transit time ( $T_{f,r,p_f}$ ). The total transit time is equal to the sum of the duration of the initial segment ( $T_{f,r,p_i}$ ), sequencing leg ( $T_{f,r,p_T}$ ) and the CDO segment ( $T_{f,r}^{CDA}$ ). It is calculated using equation 5.43.

$$A_{f,r}(T_{f,r,p_f} - T_{f,r,p_i} - T_{f,r,p_T} - T_{f,r}^{CDA}) = 0 \quad (5.43)$$

### 5.5.8 Fuel Consumption Constraint

In order to compute the fuel consumption, the equations described in section 3 are used. Due to the non-linearity of the fuel rate an approximation has to be done. Two linear functions, where the slope changes halfway the feasible velocity range, called a special ordered set will be the approximation of the fuel rate. This approximation is as shown in equation 5.44.

$$FR_{f,r} = \begin{cases} (\alpha_{f,r}^1 V_{LEG_{f,r}} + \beta_{f,r}^1) \text{ for } V_{f,r,p}^{min} \leq V_{LEG_{f,r}} \leq \frac{V_{f,r,p}^{max} - V_{f,r,p}^{min}}{2} \\ (\alpha_{f,r}^2 V_{LEG_{f,r}} + \beta_{f,r}^2) \text{ for } \frac{V_{f,r,p}^{max} - V_{f,r,p}^{min}}{2} \leq V_{LEG_{f,r}} \leq V_{f,r,p}^{max} \end{cases} \quad (5.44)$$

In order to convert the fuel rate, which is in kilograms per nautical mile, to the fuel used in kilograms, the next equation is introduced:

$$Z_{LEG_{f,r}} = FR_{f,r} d_{f,r}^{turn} \quad (5.45)$$

And by substituting it in equation 5.45 we obtain:

$$Z_{LEG_{f,r}} = \begin{cases} (\alpha_{f,r}^1 V_{LEG_{f,r}} + \beta_{f,r}^1) d_{f,r}^{turn} \text{ for } V_{f,r,p}^{min} \leq V_{LEG_{f,r}} \leq \frac{V_{f,r,p}^{max} - V_{f,r,p}^{min}}{2} \\ (\alpha_{f,r}^2 V_{LEG_{f,r}} + \beta_{f,r}^2) d_{f,r}^{turn} \text{ for } \frac{V_{f,r,p}^{max} - V_{f,r,p}^{min}}{2} \leq V_{LEG_{f,r}} \leq V_{f,r,p}^{max} \end{cases} \quad (5.46)$$

For simplicity  $V_{LEG_{f,r}} = \frac{A_{f,r}T_{f,r,P_T}}{d_{f,r}^{turn}}$  is substituted into equation 5.46 and equation 5.47 is obtained:

$$Z_{LEG_{f,r}} = \alpha_{f,r}^1 A_{f,r} T_{f,r,P_T} + \beta_{f,r}^1 d_{f,r}^{turn} \quad (5.47)$$

This same approach is also used for the fuel calculation in the initial segment and the calculation of the fuel used during the continuous descent approach segment is computed in the performance calculations of section 3. With all of this, the total fuel used is computed by equation 5.48:

$$Z_{f,r,P_F} - Z_{f,r,P_i} - Z_{LEG_{f,r}} - Z_{CDO_{f,r}} = 0 \quad (5.48)$$

## CHAPTER 6. PERFORMANCE ANALYSIS

A day traffic study based on real traffic data of the Berlin-Schönefeld Airport is performed. Data of all the incoming flights at this airport on the 10<sup>th</sup> August 2017 has been gathered through DDR2 (Demand Data Repository 2). DDR2 is a service from Eurocontrol that provides the most accurate picture off pan-European air traffic demand, past and future. Thanks to this service we can access the historical traffic.

The data obtained contains all incoming flights from each of the IAFs for the entire day from the top of descent to the runway. Every flight is constituted by a set of position coordinates and a time stamp at each position.

From the information gathered, 26 different aircraft types can be differentiated in the data set. In figure 6.1 and 6.2 it can be seen the resulting aircraft mix and size.

### Aircraft Type Distribution

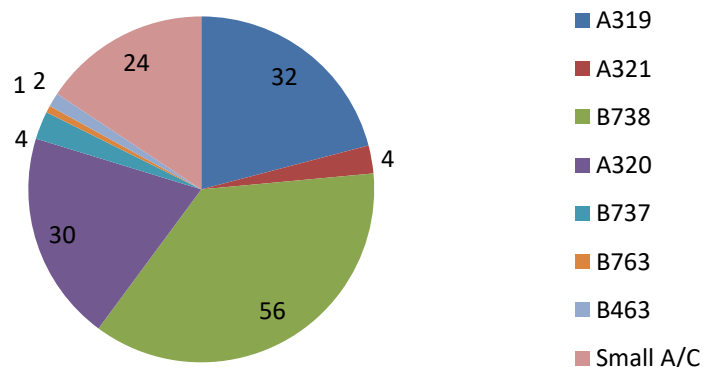


Figure 6.1: Aircraft mix on 10th August, 2017, at Berlin Schönefeld

It has been observed that during the analyzed day, the Boeing 737 and other aircraft comparable in terms of mass, dimensions and performance such as Airbus A320 represent the majority of all arriving aircraft. Therefore, Airbus A320 has been selected as the representative aircraft for this study.

## Aircraft Size Distribution

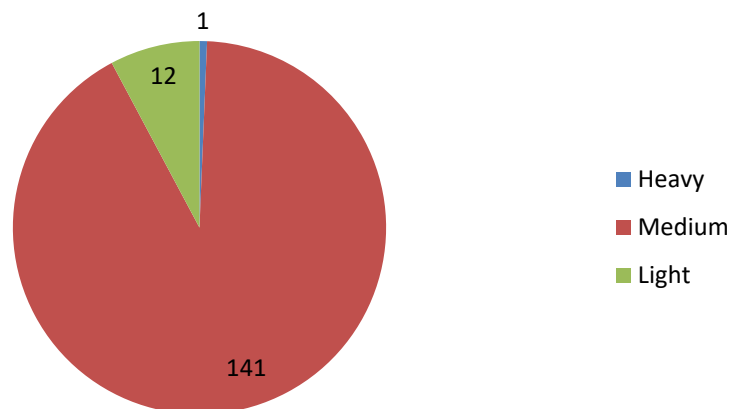


Figure 6.2: Aircraft size on 10th August, 2017, at Berlin Schönefeld

It can be observed that the most common aircraft type is the B738 and the aircraft type of weight “Large (Medium)” predominate the normal day traffic of the airport being them almost the 92% of the aircraft type flying to Berlin-Schönefeld.

The flight data set obtained from DDR2 consists of 154 incoming aircraft. The flight arrival distribution along the day can be graphically seen in figure 6.3.

## Number of flights

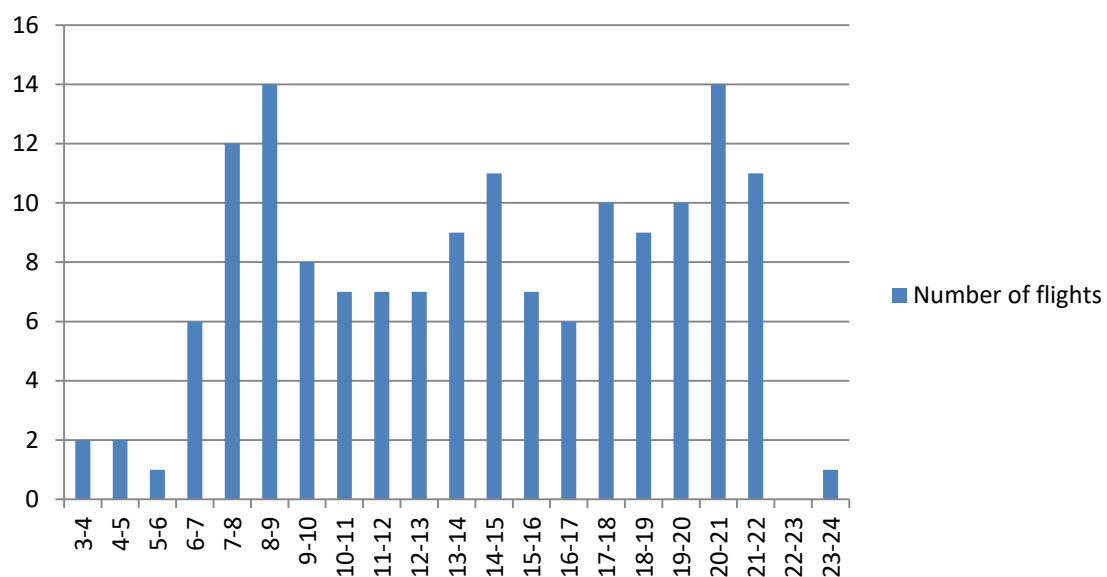


Figure 6.3: Aircraft time distribution on 10th August, 2017, at Berlin Schönefeld

Regarding at this figure three peaks of arrivals can be identified. The first one at the morning, the second one during midday, and the third one at the evening; being the second one a little smaller than the other two.

Berlin-Schönefeld is not one of the busiest airports in Europe, having only 154 arrival flights in the middle of the summer season and its peaks being not very remarkable. Being the maximum peak 14 aircraft per hour we can expect a not so difficult management of the incoming traffic using the PM procedure due to its flexibility to sequence and merge the aircraft. Even if the traffic was higher a PM procedure should be able to cope with it and manage it correctly and efficiently.

## 6.1 Graphic Outputs

Once the theoretical study has been completed we can move on to this section in which we will explain the trajectory optimizer written in Python that is used to generate the CDO profile each aircraft will fly. These profiles obtained by the program will be analyzed and discussed.

As seen before, from the data extracted, 26 different aircraft types are found in the data set. Because not all aircraft types are available in BADA, it has been decided to approximate the performance of six aircraft models that represent a normal day of traffic: A320-231, EMB-135ER, B773RR92, B737W24, B738W26 and A340-313.

For each aircraft we will study different cases depending on the mass of it and the cost index assigned to it. So four different masses will be assessed for each aircraft, from the aircraft at full weight to the aircraft at minimum weight, and five different cost indexes will also be evaluated, from CI 0 to CI 100. A speed of 220kts, which is the speed limit at the PM as stated in chapter 5, has been selected and a distance has also been selected for each type of aircraft.

These will be the input data for the program that by using the BADA information from Eurocontrol for each type of aircraft will compute the CDO profiles and will generate a csv file which contains all the information related to the profile: (time, distance, altitude, velocity and fuel).

With these outputs we can easily plot the information we need to assess the CDO profiles. We will plot speed vs altitude, distance vs time, distance vs altitude and fuel consumption which are the most relevant information we can get.

These plots will help us to see the performance of the aircraft during the descent in the PM and how the parameters mentioned above affect it. These will allow us to confirm that a PM procedure could be performed by all these aircraft flying within the restrictions stipulated in chapter 3.

### 6.1.1 Speed vs Altitude

The first output we are going to obtain is the speed vs altitude plot. For this plot there has been no limitation on the velocity in order to get a good view of a continuous descend from cruise level to runway.

In these plots we can observe the optimal velocity curve for each flight in between the Green Dot speed (which is the best lift to drag speed) and the Maximum Operating speed (which is, as its name says, the maximum permitted speed for an aircraft).

Next, some plots will be shown to discuss the differences, first we will see the speed vs altitude plots of an A320-231 with MTOW but different cost index.

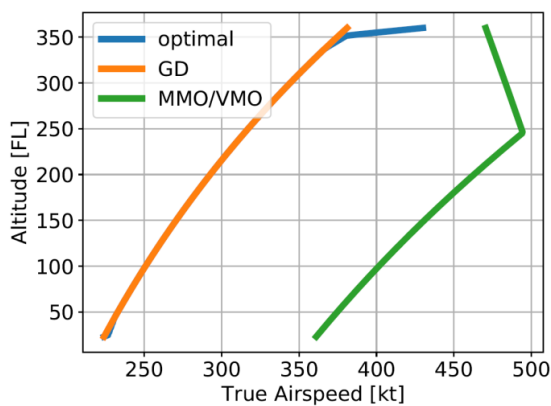


Figure 6.4: A320 MTOW C.I. 0 speed vs altitude.

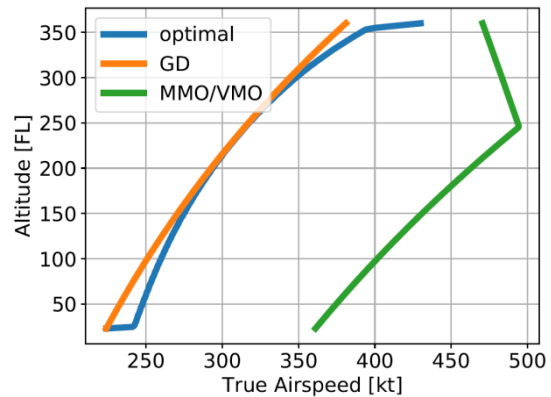


Figure 6.5: A320 MTOW C.I. 20 speed vs altitude.

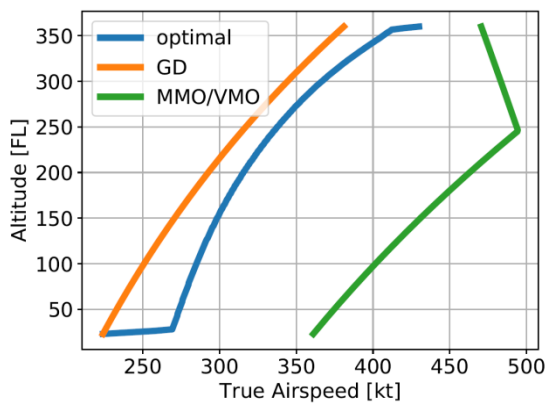


Figure 6.6: A320 MTOW C.I. 40 speed vs altitude.

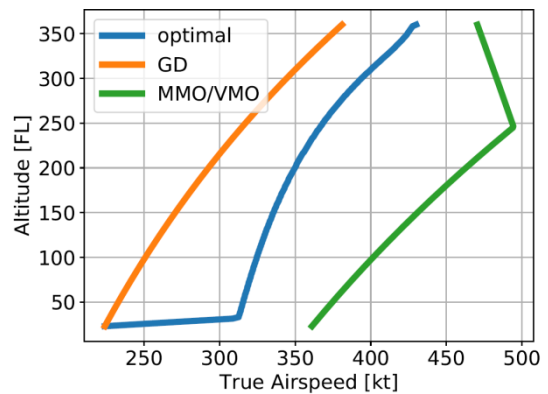
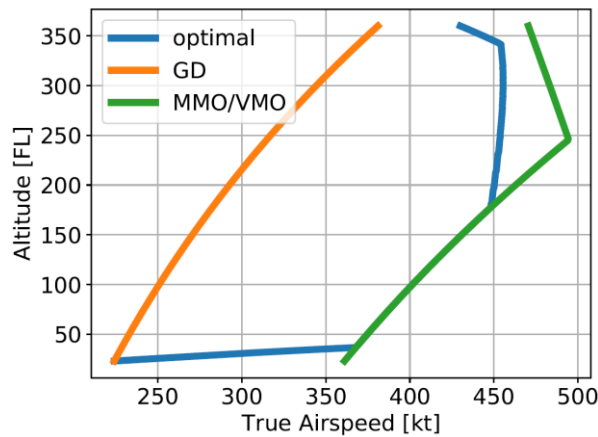


Figure 6.7: A320 MTOW C.I. 60 speed vs altitude.



**Figure 6.8: A320 MTOW C.I. 100 speed vs altitude.**

In the first plot (figure 6.4), which corresponds to a flight flying with cost index 0, we can observe that the aircraft follows as soon as possible the Green Dot speed which gives the best climb/descend performance and also is the most economic speed so the aircraft will consume less fuel.

We can appreciate that as the cost index is incremented the speed of the descent is greater which means that the aircraft flies faster in order to land earlier but with the drawback of consuming more fuel.

Finally, we can see in the last plot (figure 6.8), corresponding to the flight with cost index 100, that the aircraft tries to follow as soon as possible the maximum operating speed as explained before to reach the runway in the shortest time possible.

Now, to see the differences between the different masses of a flight we will take the plots of a B737 with cost index 60.

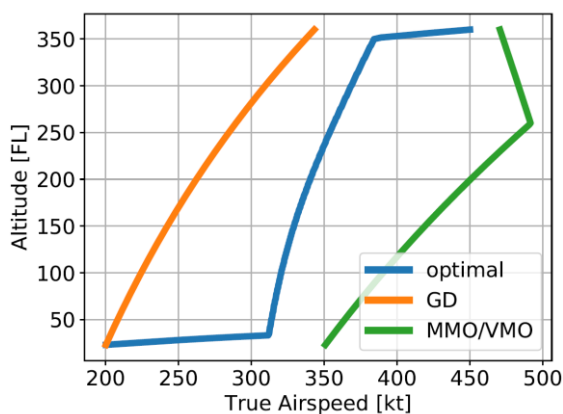


**Figure 6.9: B737 C.I. 60 mass 45250kg speed vs altitude.**

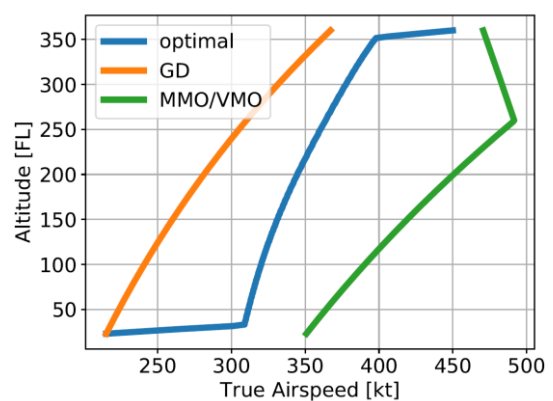


**Figure 6.10: B737 C.I. 60 mass 52650kg speed vs altitude.**

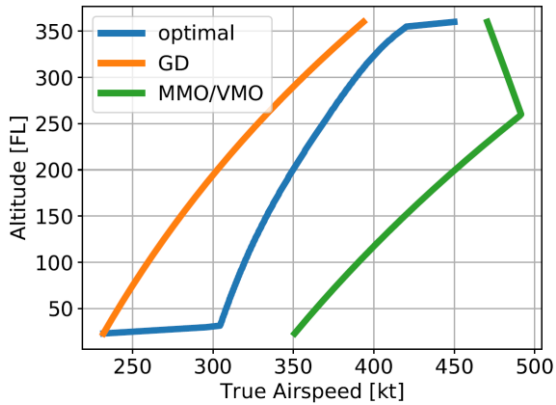


**Figure 6.11: B737 C.I. 60 mass 61615kg speed vs altitude.**

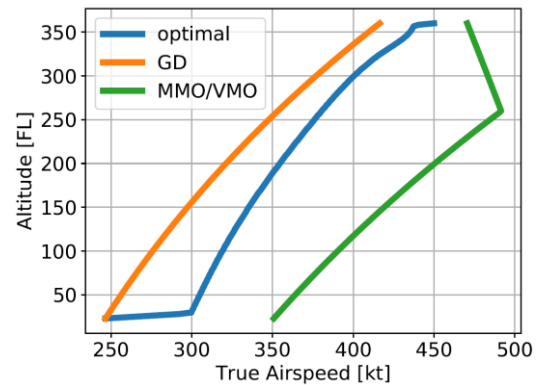


**Figure 6.12: B737 C.I. 60 mass 70080kg speed vs altitude.**

In this group of four plots it can be appreciated the effect of the mass of the aircraft. The higher the mass of the aircraft is, more closer to the green dot speed the trajectory is, and on the other hand, the lighter the aircraft is it descends at higher speed. So we can assume that when the aircraft is heavier it flies at a velocity the most closer to the green dot possible due to it being the most efficient speed with the best lift to drag ratio.

### 6.1.2 Altitude vs Distance

After discussing the speed vs altitude outputs the next step is to analyse the altitude vs distance results. These plots represent the vertical profile each flight follows. We will start by discussing the profiles of the A320-231, as explained before, with different cost indexes and masses:

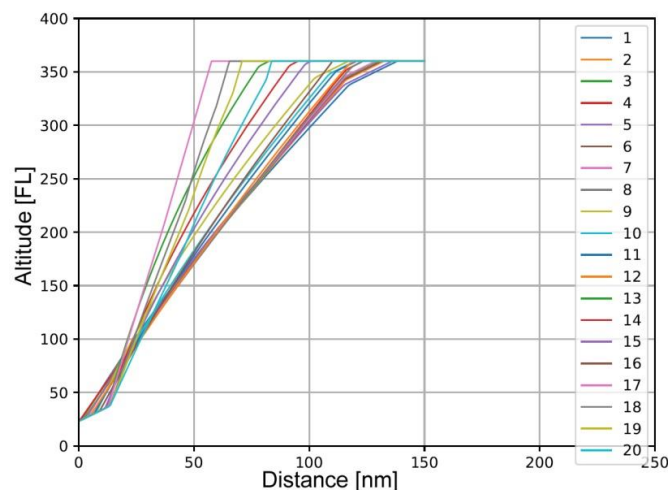


**Figure 6.13: A320-231 profiles.**

In this figure representing the vertical profiles of all the A320 cases we can see the comparison between them. It can be seen that depending on the cost index and the mass of the aircraft it will start the descent earlier or later.

Next, we will compare the profiles of two type of aircraft completely different, the EMB-135ER and the B773RR92.

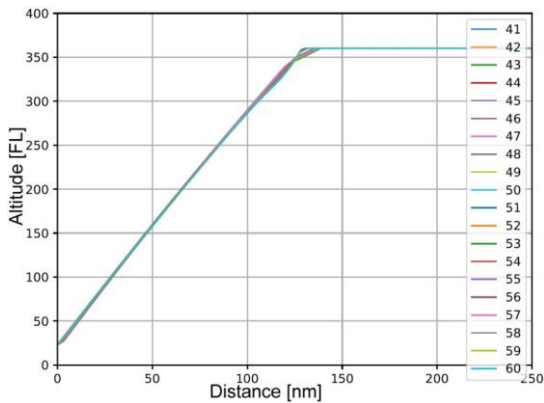


Figure 6.14: B773RR92 profiles.

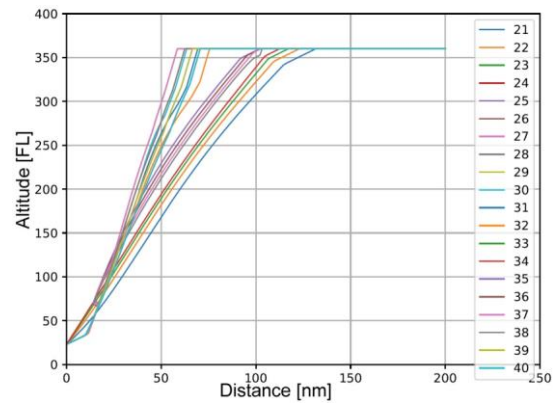


Figure 6.15: EMB-135ER profiles.

It can be seen that the profiles between these two types of aircraft are quite different; the profiles of the B773RR92 are practically identical. On the other side, the profiles of the EMB-135ER are pretty different one from each other. So it can be said that the heavier the aircraft is the less impact it has from its weight. Lighter aircraft have bigger impact in their profiles due to change of weight than bigger ones.

Next, the comparison of the profiles between different cost indexes will be performed.

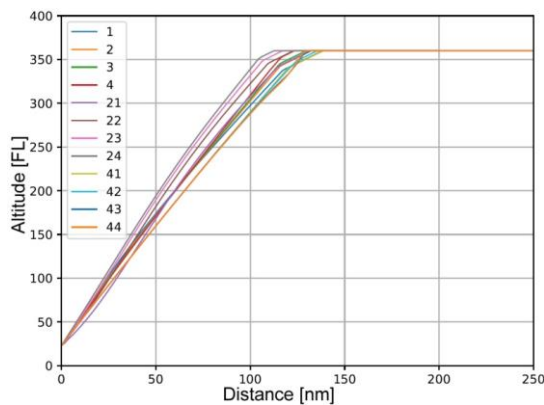


Figure 6.16: C.I. 0 profiles.

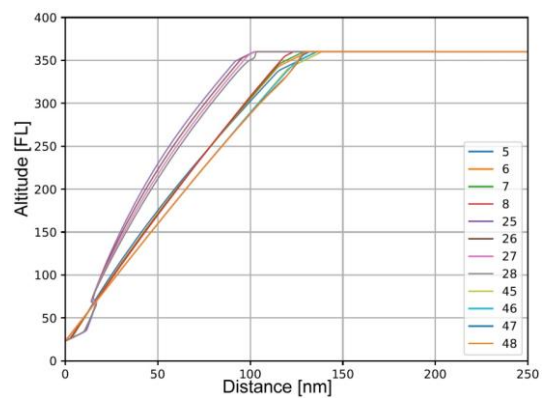


Figure 6.17: C.I. 20 profiles.

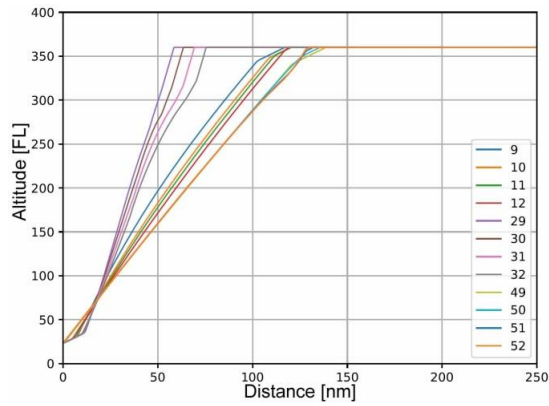


Figure 6.18: C.I. 40 profiles.

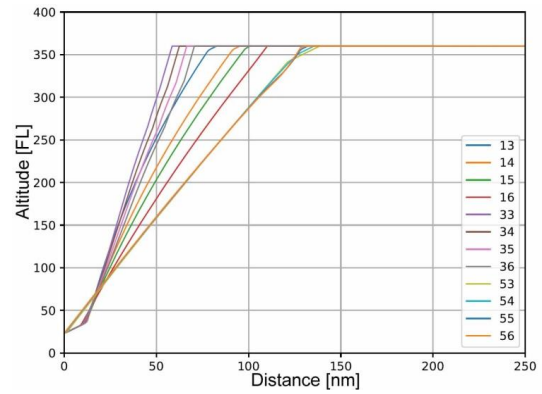


Figure 6.19: C.I. 60 profiles.

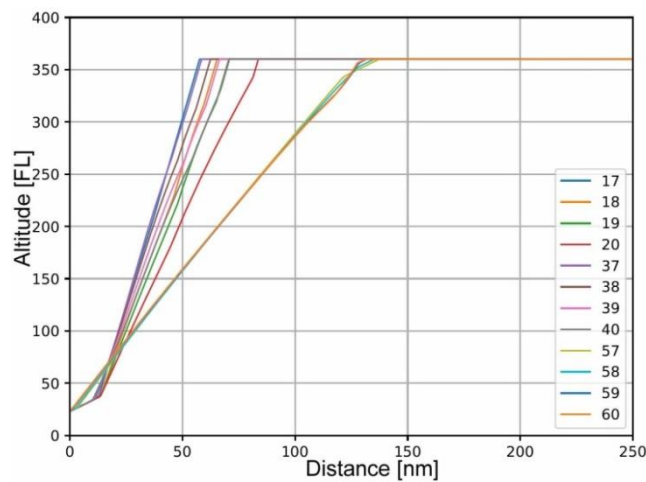


Figure 6.20: C.I. 100 profiles.

Regarding these plots, it can be said that as the cost indexes increase the start of the descent is later and the rate of descent is greater, which is reasonable because as discussed before, the higher the cost index the higher the descent speed which results in less distance of descent so the aircraft start descending closer to the runway with a higher angle of descent.

Now, the profiles of the aircraft with different masses will be showed and analyzed.

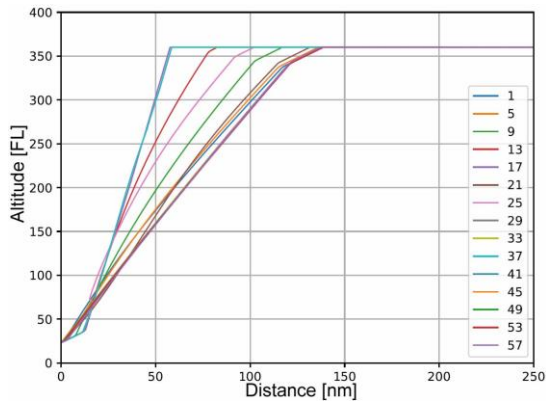


Figure 6.21: Load 0% profiles.

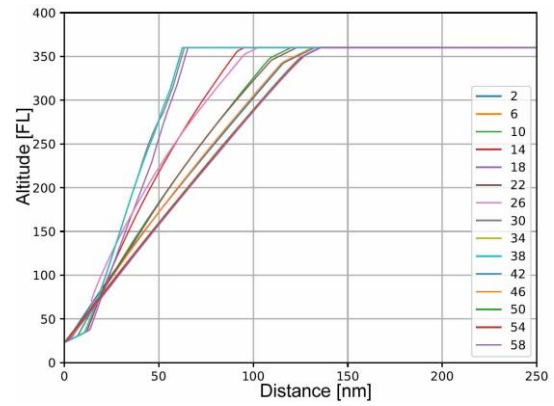


Figure 6.22: Load 33% profiles.

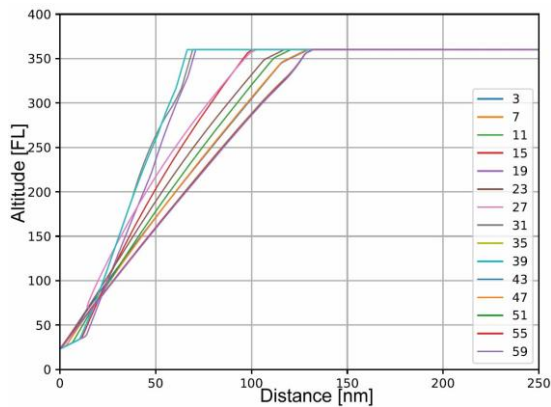


Figure 6.23: Load 66% profiles.

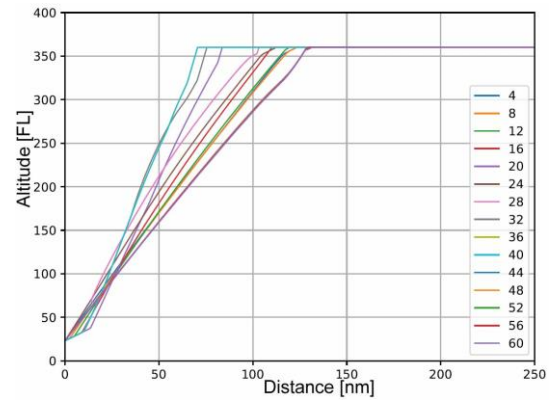


Figure 6.24: Load 100% profiles.

Looking at these plots comparing the different aircraft weights it can be observed that as the aircraft gets heavier it starts descending earlier because it cannot descend with a high rate of descent and it needs more distance to perform the descent.

### 6.1.3 Time vs Distance

Finally, the time vs distance results will be analyzed. Again we will start by showing the A320-231 results.

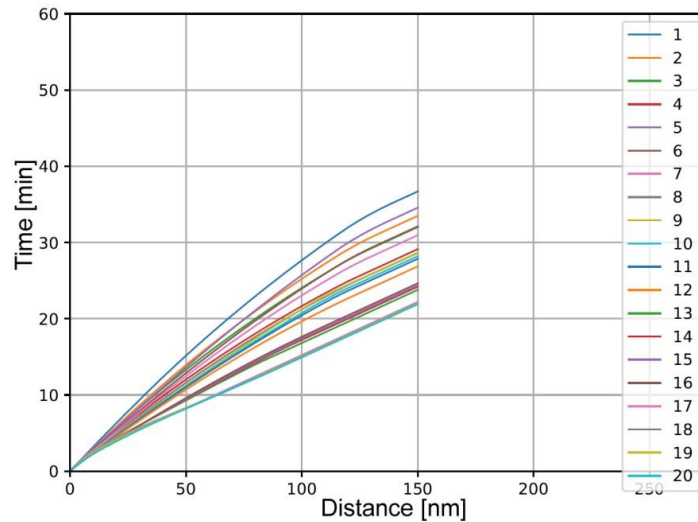


Figure 6.25: A320-231 time vs distance.

Again we can see that different results are obtained depending on the cost index and mass of the aircraft. The lower the mass and the higher the cost index the lower time the aircraft requires to arrive to the runway.

Finally, the time vs distance results separated by cost index will be showed and commented.

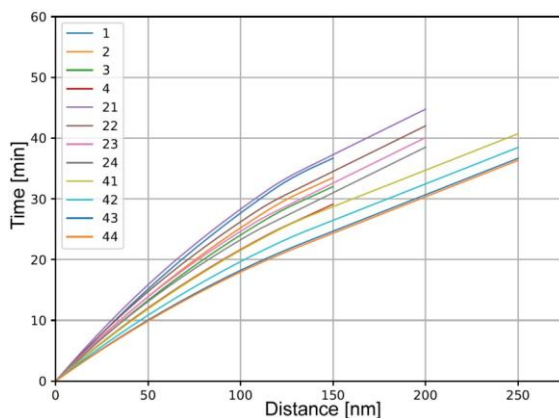


Figure 6.26: C.I. 0 time vs distance.

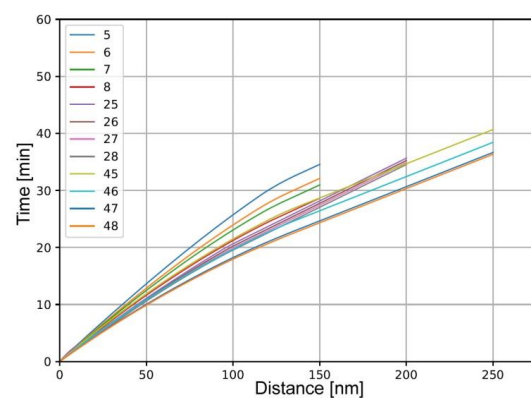
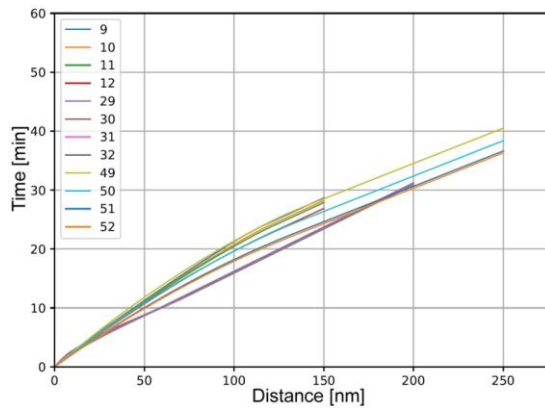
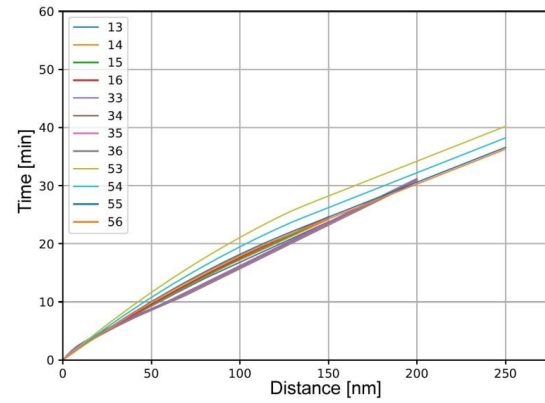


Figure 6.27: C.I. 20 time vs distance.



**Figure 6.28: C.I. 40 time vs distance.**



**Figure 6.29: C.I. 60 time vs distance.**

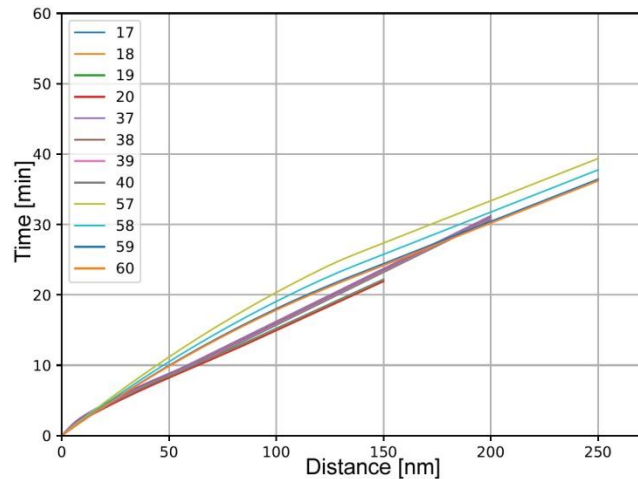


**Figure 6.30: C.I. 100 time vs distance.**

By looking at these graphics it can be observed that as the cost index increases the time of descent decreases which is exactly what we stated at the beginning of this section, that the higher the cost index the aircraft flies at a higher speed reaching the runway in less time that the aircraft flying at lower cost indexes.

#### 6.1.4 Fuel consumption

Now it is time to analyze the results of fuel consumption of our simulated flights and to observe the data depending on the cost index and load of the aircraft. First, we will take a look at the fuel consumption plots relative to the cost index.

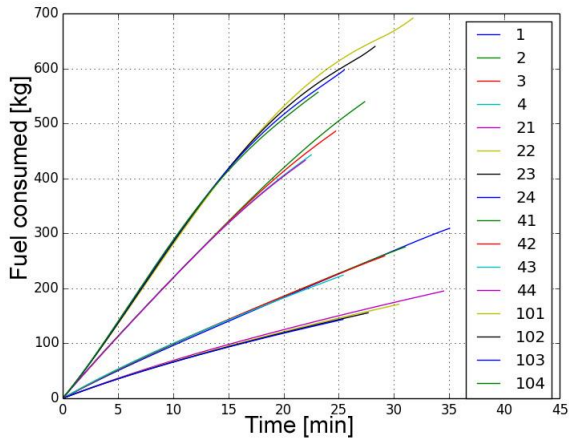


Figure 6.31: C.I. 0 Fuel consumption.

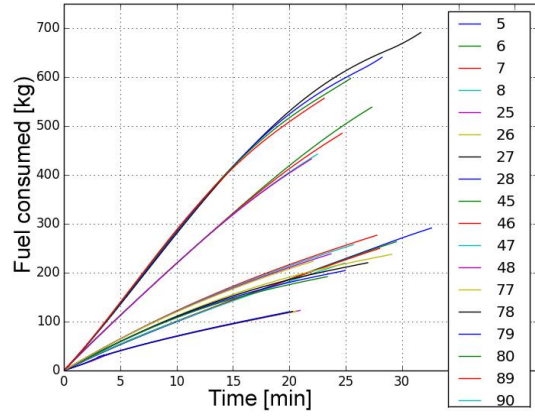


Figure 6.32: C.I. 20 Fuel consumption.

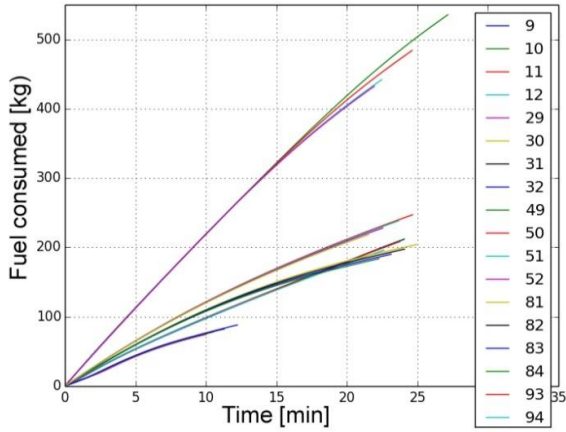


Figure 6.33: C.I. 40 Fuel consumption.

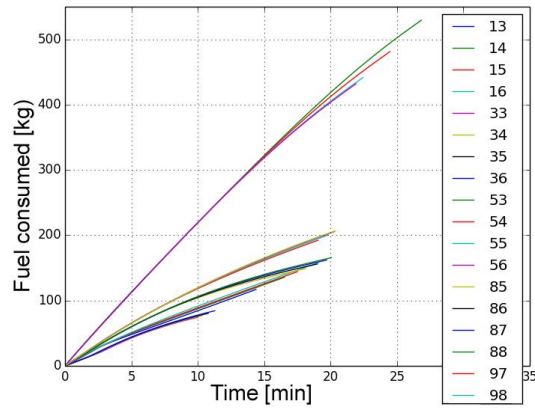


Figure 6.34: C.I. 60 Fuel consumption.

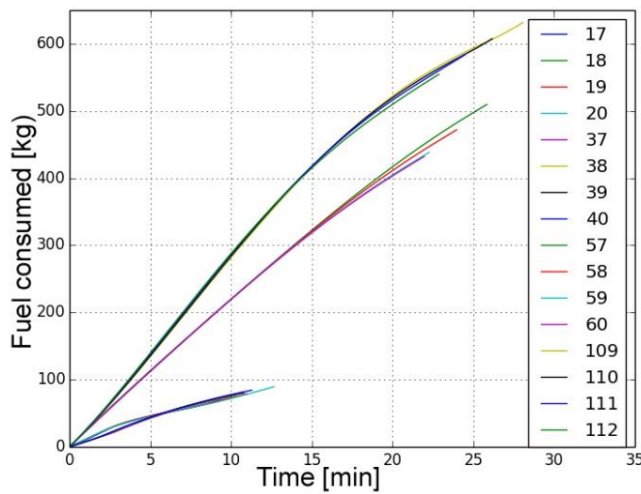
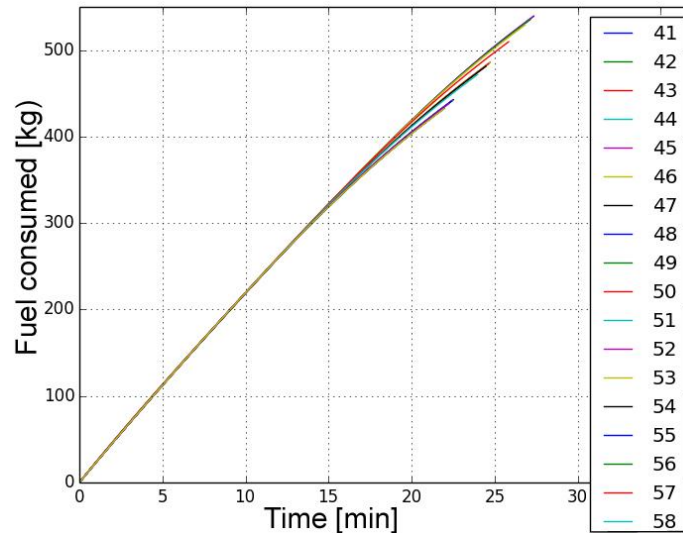


Figure 6.35: C.I. 100 Fuel consumption.

Regarding at these plots we can observe that as the cost index increases the fuel consumption increases due to the aircraft flying at a higher speed. This is highly noticed on the light aircraft (A320, EMB135, B737 and B738), but on the heavy aircraft (A340 and B773) the variation in fuel consumption is really low.

We will take a look only at the B773 fuel consumption plot:



**Figure 6.36: B773 Fuel consumption.**

Exactly as said before, the change in fuel consumption is not very much. It is true that we can appreciate the difference in between cost indexes, being the high cost indexes the flights that consume less and the low cost index the ones that consume more. But between flights of the same cost index (load is the parameter changing) the variation is practically unnoticeable.

On the other side, if we look at the results of a lighter aircraft as the A320 we obtain:

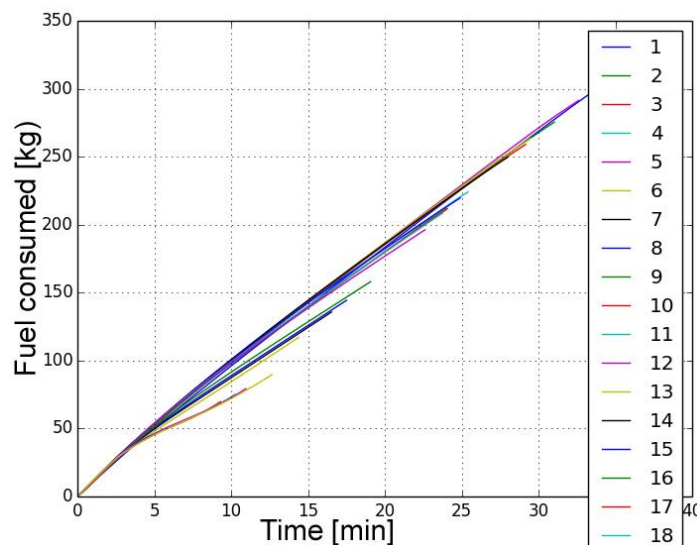


**Figure 6.37: A320 Fuel consumption.**

Observing the plot for just one type of aircraft we can appreciate the difference in fuel consumption. The flights with the same load have big differences in the fuel consumed. Whilst the flights with the same cost index have similar fuel consumption. Next, we will analyze the results separating the flights per load.

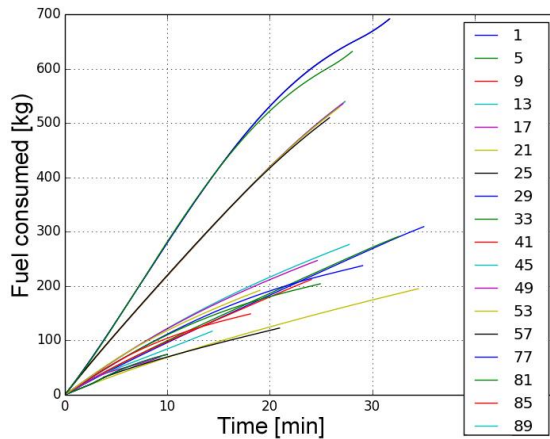


**Figure 6.38: Load 0% Fuel consumption.**

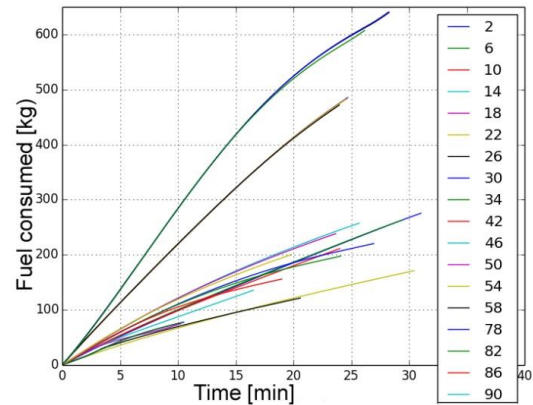


**Figure 6.39: Load 33% Fuel consumption.**

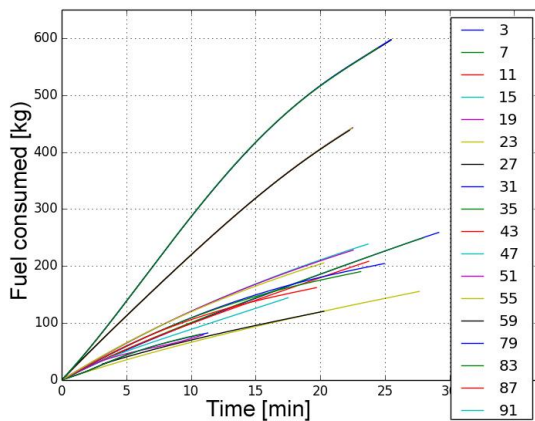


**Figure 6.40: Load 66% Fuel consumption.**

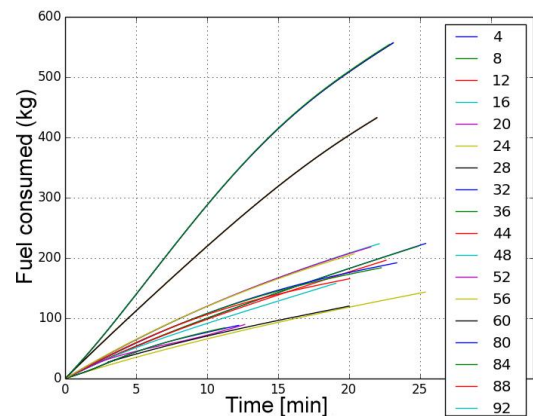


**Figure 6.41: Load 100% Fuel consumption.**

By comparing the results of the different loads it is way more remarkable the change in fuel consumption than in the previous plots. Here we can observe that as the load increases the fuel consumed decreases.

## CHAPTER 7. CONCLUSIONS

The Point Merge System is a really innovative arrival procedure developed by EUROCONTROL Experimental Centre (EEC) to merge arrival flows of aircraft. It is mainly designed for big airports due to it being able to cope with busy TMAs and high traffic loads.

The PMS procedure allows the aircraft to perform CDOs, that represent a reduction in the fuel consumed by the aircraft. It has been studied that this procedure can reduce the delay by reducing the holding times, which again reduces the fuel consumed; and since the fuel consumption is one of the greatest objectives of improvement in the aviation, this procedure is a good method for reducing the environmental impact by the aircraft.

As stated in section 2, a design of a Point Merge System has been proposed for runway 07L of the Berlin-Schönefeld airport adapting the actual arrival routes to a point merge arrival procedure. Since the incoming flow traffic for the runway 07L of Berlin-Schönefeld merges at one IAF for all the north traffic and at another for all the south traffic, the design of PMS selected has been a single Point Merge System composed by two arcs, one arc used for the incoming north traffic and the other for the incoming south traffic maintaining these two IAFs.

It can be concluded that a PMS could be implemented in the airport without major changes using existing available airspace so the PMS can have a suitable size to be able to separate and sequence all the incoming traffic flow.

To sum up, Berlin-Schönefeld is suitable for the implementation of a PMS procedure so it could benefit from its vast advantages.

The aircraft trajectories generated with a trajectory optimizer have been analyzed, assuming the performance models from BADA. It can be concluded that when the aircraft flies at a higher cost index it descends at a higher speed, which results in a lower time of descend but with the drawback of a higher fuel consumption. On the other hand, if the aircraft flies at a low cost index it will descend with a velocity near to the green dot speed. This means that the aircraft will fly with a better descend performance, which implies a more economic speed. As a result, the fuel consumption will be lower but the time of descend will be higher. Regarding the fuel consumption, it has been concluded that the higher the cost index the higher the fuel consumption and the more loaded the aircraft is less fuel it consumes. In the future implementation of the PMS at Berlin-Schönefeld, trajectories with different values of CI could be used in order to sequence and merge the traffic in the PMS and ensuring a safe separation.

To sum up, we can conclude that the airport of Berlin-Schönefeld is capable of the implementation of a PMS that would increase its ATC capacity and reduce the environmental impact of all the traffic due to a better fuel efficiency from the aircraft because they would be performing CDOs so it would result in noticeable

fuel savings for each aircraft. These improvements could be achieved without any loss of safety with a good aircraft sequencing.

## CHAPTER 8. BIBLIOGRAPHY

- [1] Eurocontrol, “Point Merge Integration of Arrival Flows Enabling Extensive RNAV Application and CDA Operational Services and Environment Definition”, Eurocontrol Experimental Center, 2010
- [2] R. Dalmau, J. Alenka, and X. Prats, “Combining the assignment of pre-defined routes and RTAs to sequence and merge arrival traffic,” in *17th AIAA Aviation Technology, Integration, and Operations Conference (ATIO)*, Denver, CO, 2017
- [3] “Point Merge: improving and harmonising arrival operations with existing technology.”  
<http://www.eurocontrol.int/services/point-merge-concept>. [Accessed January 1<sup>st</sup>, 2019]
- [4] J.M. de Wilde, “Implementing point merge system based arrival management at Amsterdam Airport Schiphol”. Master Thesis. Delft University of Technology, Delft, 2018
- [5] D. Ivanescu, C. Shaw, C. Tamvaclis, and T. Kettunen, “Models of Air Traffic Merging Techniques: Evaluating Performance of Point Merge,” in *9th AIAA Aviation Technology, Integration, and Operations (ATIO) Conference*, Hilton Head, South Carolina, September, 2009
- [6] M. Liang, D. Delahaye, and P. Maréchal., “A Framework of Point Merge-based Autonomous System for Optimizing Aircraft Scheduling in Busy TMA” in *5th SESAR Innovation Days*, Bologna, 2015
- [7] R. Sáez, R. Dalmau, and X. Prats, “Optimal assignment of 4D close-loop instructions to enable CDOs in dense TMAs” in *Digital Avionics and Systems Conference (DASC)*, London, 2018
- [8] M. Samà, A. D’Ariano, and D. Pacciarelli., “Rolling Horizon Approach for Aircraft Scheduling in the Terminal Control Area of Busy Airports” in *20th International Symposium on Transportation and Traffic Theory (ISTTT)*, 2013
- [9] H. Balakrishnan, and B. Chandran. “Scheduling Aircraft Landings under Constrained Position Shifting” in *AIAA Guidance, Navigation and Control Exhibit*, Keystone, CO, 2006
- [10] Eurocontrol Experimental Centre, “User Manual for the Base of Aircraft Data (BADA) revision 3.8”, 2010.
- [11] Eurocontrol, “Continuous Climb and Descent Operations”.  
<https://www.eurocontrol.int/articles/continuous-climb-and-descent-operations>  
[Accessed January 16<sup>th</sup>, 2019]